6-18-2021

Development of Novel Low-Cost Rapid Tooling Solution by Incorporating Fused Deposition Modeling Sacrificial Patterns

Alireza Davoud Pasha
University of Windsor

DEVELOPMENT OF NOVEL LOW-COST RAPID TOOLING SOLUTION BY INCORPORATING FUSED DEPOSITION MODELING SACRIFICIAL PATTERNS

By

Alireza Davoud Pasha

A Thesis

Submitted to the Faculty of Graduate Studies

through the Department of **Mechanical, Automotive & Materials Engineering**

in Partial Fulfillment of the Requirements for
the Degree of Master of Applied Science
at the University of Windsor

Windsor, Ontario, Canada

2021

DEVELOPMENT OF NOVEL LOW-COST RAPID TOOLING SOLUTION BY INCORPORATING FUSED DEPOSITION MODELING SACRIFICIAL PATTERNS

by

Alireza Davoud Pasha

APPROVED BY:

_____

N. Biswas
Department of Civil and Environmental Engineering

_____

J. Johrendt

Department of Mechanical, Automotive & Materials Engineering

_____

J. Urbanic, Co-advisor

Department of Mechanical, Automotive & Materials Engineering

_____

O. Jianu, Co-advisor

Department of Mechanical, Automotive & Materials Engineering

April 8, 2021

DECLARATION OF CO-AUTHORSHIP AND PREVIOUS PUBLICATION

I. Co-Authorship

I hereby declare that this thesis incorporates material that is result of joint research, as follows:

> Chapter 3.1 of this thesis contains design ideas that were developed as a team effort by Dr. Hamed Kalami, Morteza Alebooyeh, Mohamad Najimi, Hamoon Ramezani and Alireza D. Pasha. Additionally, Chapter 3.2.2 of this thesis contain information co-authored by Hamoon Ramezani. The research is performed under the supervision of Dr. Jill Urbanic and Dr. Ofelia Jianu. In all cases, application, and adaptation of previous research contents to this thesis is done by the author, under the supervision of Dr. Jill Urbanic and Dr. Ofelia Jianu. Bob Hedrick provided additional technical insight for development of this project.

I am aware of the University of Windsor Senate Policy on Authorship and I certify that I have properly acknowledged the contribution of other researchers to my thesis, and have obtained written permission from each of the co-author(s) to include the above material(s) in my thesis.

I certify that, with the above qualification, this thesis, and the research to which it refers, is the product of my own work.

II. Previous Publications

This thesis includes one original paper that has been previously published/submitted for publication in peer reviewed journals, as follows:

Chapter	Publication title/full citation	Publication Status
Chapters 3 & 4	Davoud Pasha, A., Urbanic, J., Hedrick, B., Ramezani, H., Jianu, O. (2021) *Leveraging Advanced Design and Novel Rapid Manufacturing Solutions to Respond to the COVID19 Pandemic*, Computer-aided design, and applications Journal	Accepted

I certify that I have obtained a written permission from the copyright owner(s) to include the above published material(s) in my thesis. I certify that the above material describes work completed during my registration as a graduate student at the University of Windsor.

III. General

I declare that, to the best of my knowledge, my thesis does not infringe upon anyone's copyright nor violate any proprietary rights and that any ideas, techniques, quotations, or any other material from the work of other people included in my thesis, published or otherwise, are fully acknowledged in accordance with the standard referencing practices. Furthermore, to the extent that I have included copyrighted material that surpasses the bounds of fair dealing within the meaning of the Canada Copyright Act, I certify that I have obtained a written permission from the copyright owner(s) to include such material(s) in my thesis.

I declare that this is a true copy of my thesis, including any final revisions, as approved by my thesis committee and the Graduate Studies office, and that this thesis has not been submitted for a higher degree to any other University or Institution.

ABSTRACT

Injection molding and additive manufacturing (3D-printing) are two manufacturing solutions that are suitable to produce plastic components. The material extrusion-based additive manufacturing (AM) process deposits beads side by side through an extrusion to build prototypes. This process is capable of manufacturing complex geometries, but it is very expensive and slow. As a result, it is not the best solution for manufacturing low to medium (10-5000) production volumes. Additionally, there are limited materials for AM as compared to injection molding. Injection molding process is very fast, reliable, and low-cost to produce thousands of a single product in a short time. However, the initial investment for building the mold is very high and it may take up to several weeks to manufacture a good quality mold. To cover the gap between these two processes, a low-cost tooling solution with a reduced build time has been developed that is suitable for low to medium production. Internal features are integrated within the tooling to investigate the possibility of building internal channels that can later be optimized to improve the cooling efficiency of the tool. The developed tooling solution was designed for a hands-free door handle. Design for manufacturing (DfM) strategies were applied to the initial CAD design to make it suitable for an injection molding process. Finite element analysis (FEA) and injection molding simulations were used to conduct virtual studies on this low-cost tooling solution. To create the internal features, soluble material (SR-30 developed by Stratasys) was used and Aremco 805 epoxy was cast to create the mold cavities. After curing the epoxy, the soluble patterns were dissolved to create the final mold. The developed tooling was able to manufacture the J-hook with a dimensional precision of approximately 1% - 3% of the desired geometries. Additionally, no sink mark or shrinkage was observed on the surfaces of the final product. Most importantly, the cost of the solution was kept under 500 CAD dollars and complex internal features were built without any additional support structure on the inside. Build time of the J-hook was reduced from 3 hours to less than 2 minutes and most importantly, the piece price of each J-hook was lowered by more than 44 CAD dollars per piece.

DEDICATION

I want to dedicate to my parents, whose unconditional love and support enabled me to follow my goals and passion in my life as well as my academic career.

ACKNOWLEDGEMENTS

First of all, I would like to sincerely thank my supervisors, Dr. Jill Urbanic and Dr. Ofelia Jianu for their guidance and help during my research and studies and without their help, I would not have been able to complete this research.

I would like to thank Bob Hedrick and the CAMufacturing family for accepting me as their intern during my master's studies. I have enjoyed every second of my internship and have learned a lot from this professional team.

Finally, I would like to give special thank to the COVID-19 team at University of Windsor, Dr. Hamed Kalami, Morteza Alebooyeh, Hamoon Ramezani and Mohamad Najimi for their contributions and dedication during the COVID-19 pandemic projects.

TABLE OF CONTENTS

LIST OF TABLES

LIST OF FIGURES

LIST OF APPENDICES

LIST OF ABBREVIATIONS/SYMBOLS

ABS	*Acrylonitrile Butadiene Styrene*
AM	*Additive Manufacturing*
CAD	*Computer-Aided Design*
CAM	*Computer-Aided Manufacturing*
CCC	*Conformal Cooling Channels*
FDA	*Food and Drug Administration*
FDM	*Fused Deposition Modeling*
IM	*Injection Molding*
OEM	*Original Equipment Manufacturer*
PC	*Polycarbonate*
PC-ABS	*Polycarbonate- Acrylonitrile Butadiene Styrene*
PPE	*Personal Protective Equipment*

CHAPTER 1
INTRODUCTION

Coronavirus disease refers to a range of diseases from the common cold to more severe illnesses like SARS (severe acute respiratory syndrome) and MERS (Middle East respiratory syndrome). The new coronavirus disease is referred to as COVID-19 [1]. This virus was and remains highly contagious and is easily transmitted by respiratory droplets, direct contact with infected persons or contact with contaminated objects and surfaces [2]. In late 2019, COVID-19 turned into a global pandemic that plunged the world into unprecedented times. On January 25th, Canada confirmed its first case of COVID-19. The death tolls rose and a huge demand for personal protective equipment (PPE) was created. As a result, PPE producers and suppliers were not able to deliver. At the time of this research, there was no vaccine available for this pandemic and the main ways this virus could be prevented from spreading were:

- social distancing and proper use of PPE, such as face masks and face shields, and
- eliminating the potential of transmission of virus particles to one's face as a result of touching infected surfaces.

Respiratory droplets can land on surfaces and objects. It is possible that a person could get COVID-19 by touching a surface or object that has the virus on it and then touching their mouth, nose, or eyes [3]. Public health officials have suggested that it would be safer if people were able to reduce the number of times, they touch their faces and keep their hands washed regularly. In this research, the high-level goal was to reduce the disease vectors. To achieve this, a special hands-free door handle was developed so that minimal contact is required to open/close doors. At the same time, a concurrent study was carried out to produce low-cost yet effective PPE.

Injection molding (IM) and additive manufacturing (AM) were among the processes that are capable of fabricating the products developed in this research. However, each process has its advantages and disadvantages. In the following sections, the processes, capabilities, and limitations of each process are discussed.

1.1 Injection Molding (IM)

Injection molding is one of the most commonly used manufacturing methods to fabricate plastic components. In this process, molten plastic is injected with high pressure into a mold that shapes the final geometry of the product. Once the material is fully solidified, it is ejected out of the mold and the process starts again (see Figure 1.1). A conventional IM machine has a control unit, a set of molds, and a temperature control module [4]. In addition to the main components, cooling systems, tie bares, and core slides are also crucial parts of an injection machine.

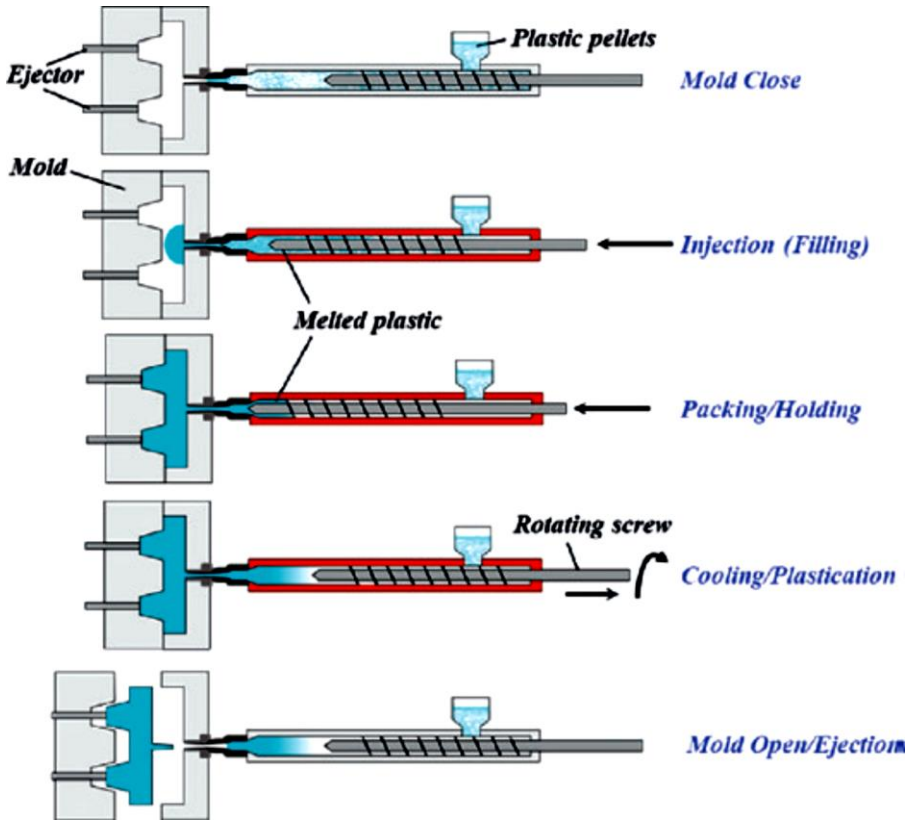

Figure 1.1 Schematic of an injection modeling process [4]

Cooling systems are a critical part of an IM process and highly affect the economics and operation of the mold. Cooling systems include a series of channels inside the mold where a coolant circulates the mold to remove the heat, and boosts solidification of the molten plastic. Figure 1.2 highlights the importance of the cooling process in an IM cycle. Like any other manufacturing process, production time and cost are strongly correlated. The

longer it takes to fabricate a part, the higher are the costs [5]. Consequently, improving the cooling system will reduce production costs.

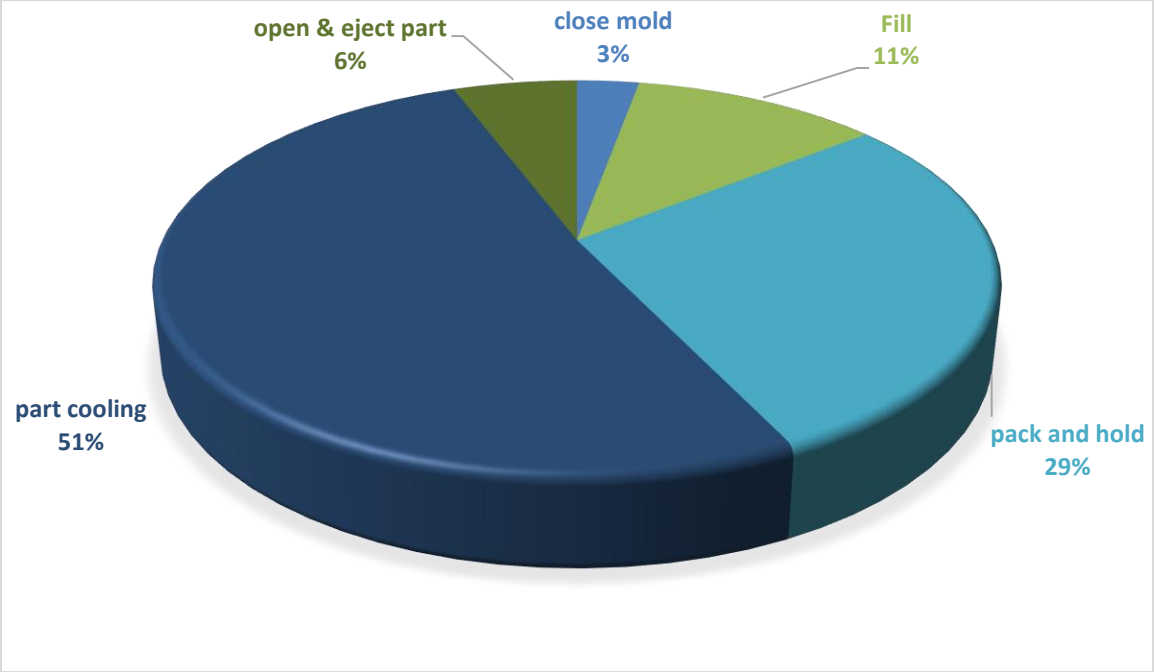

Figure 1.2 Cycle time in injection molding [5]

In addition to the cooling systems, the design of the product plays an important role in an IM process. Components with variable wall thickness should be avoided. Since the thick and thin wall sections will cool down with different cooling rates; and the variations in the cooling rates lead to quality (and potential scrap) issues [6]. Clearly, by using the same material, areas with thicker walls would take more time to cool than the thinner wall sections which could be cooled relatively faster. The different cooling rates can lead to warpage, shrinkage, or internal voids (see Figure 1.3). To maintain a more uniform structure, it is advised to use vertical ribs in areas where more stiffness is required [6]. (see Figure 1.4)

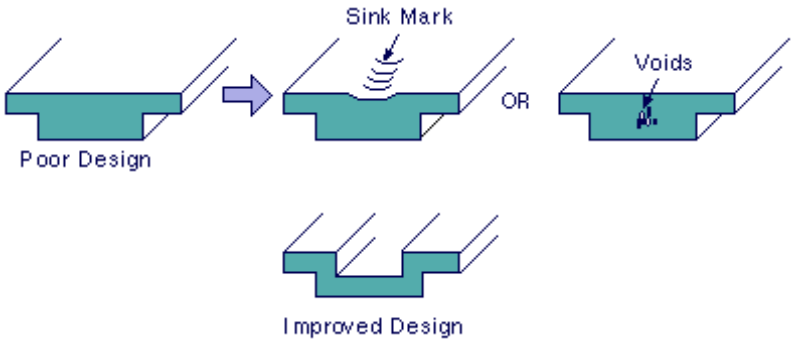

Figure 1.3 Defects caused by thick-wall design in an injection molded product [7]

Figure 1.4 Comparison of a uniform thicker part to the thinner and ribbed design [6]

One of the major challenges of IM is the initial investment in building the mold. Machining a high-quality mold costs thousands of dollars and can take up to several weeks to be finished. Additionally, manufacturing cooling channels inside a mold is highly restricted to the linear nature of machining and this limits the freedom in designing an efficient cooling system. With the advancement of AM technologies, building an object with complex internal features has been made possible. AM technologies can fabricate a product without tooling. However, metallic AM technologies can be used to fabricate a tool that is capable of building thousands of the same product. Due to the layer-by-layer nature of AM, it can create internal features inside a component. For example, it is able to build cooling channels inside a mold; however, there might be some issues. An overview of AM processes, opportunities, and limitations of AM are discussed in the next section.

1.2 Additive Manufacturing (AM)

AM (3D-printing) or layered manufacturing refers to a series of production methods where a geometry, component, or assembly is created in layers from the bottom up. This technology is the opposite of conventional subtractive manufacturing where the material is removed from a block to create the desired shape. ISO/ASTM 52900 divides the AM technologies into seven different categories and the summary of each process family is presented in Table 1.1 [8]. In this study, the material extrusion process or better known as fused deposition modeling (FDM) technology, has been used. The FDM process is further discussed in detail in section 2.1 .

Table 1.1 Summary of the AM process families (H: High, M: Medium, L: Low)

Process	Initial state	Transformation	Surface quality	Strength	Speed	Limited operator interactions	Cost
Vat photopolymerization	Liquid	Laser (and curing)	H	L	L	L	M
Material extrusion such as fused deposition modeling (FDM)	Thermoplastic wire	Resistance heater	M	M	M	L	L
Directed energy deposition	Metal wire or powder	Laser	L	H	H	H	H
Material jetting,	Liquid droplets	Liquid droplets and laser curing	H	M	M	L	M
Binder jetting,	Powder material	Liquid binder and curing	H	L	L	L	L
Powder bed fusion	Powder material	Laser	M	H	L	L	H
Sheet lamination	Solid sheets with adhesive	Laser cutting	?	?	H	L	?

To build a component via AM technologies, initially ‘water-tight’ or manifold 3D geometry is created in a computer-aided design (CAD) package. Then the file is converted into the standard tessellation language/stereolithography language (STL) format. The surface faces are converted into sets of triangles, and the triangle vertices and the face normal vectors are stored in this format. The STL file is sliced into layers and each layer is fabricated individually [9]. Each individual layer is stacked on top of the previous layer

until the final 3D geometry is created. This process is almost similar across all AM technologies. Figure 1.5 shows the process flow of AM from CAD to the actual product.

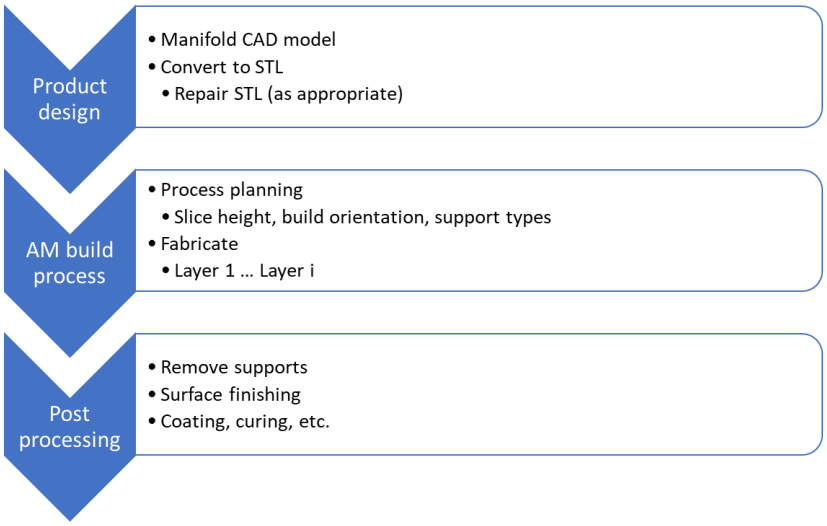

Figure 1.5 CAD to product process flow

In most AM technologies (metal, liquid, or plastic), when the geometry of the component contains overhang features with angles greater than a critical value (for example, 45°), support structures are required to be built along with the product. Support structures are necessary to create a platform for the following layers so that the subsequent layers would not collapse when deposited. Figure 1.6 shows the necessity of support structures in AM. The red lines represent the layers that make up the main component, and the green layers show the support structure.

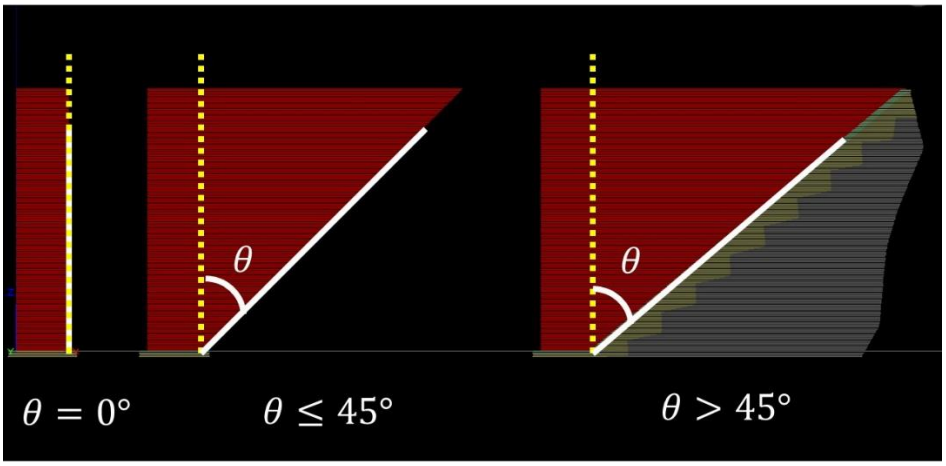

Figure 1.6 Necessity of support structure when the overhang angle exceeds a critical value (45 degrees)

1.3 Problem Statement

As explained in section 1.1 IM is a capable solution for high volume manufacturing of plastic components. However, building a mold is very expensive and usually takes up to several weeks to be completed. As a result, high production is required to justify the initial investment in building the mold. The high cost of a mold restricts IM for low to medium production. Besides, fabricating effective internal cooling channels by conventional machining is very hard and is fairly limited due to geometrical limitations. Only straight channels can be fabricated by drilling and machining. Consequently, it is very difficult to manufacture complicated three-dimensional channels, especially close to the wall of the mold (see Figure 1.7). This will lead to an ineffective cooling system because the heat cannot be removed uniformly from the mold and varying temperatures can cause warpage, distortion, and long cooling cycles. Conformal cooling channels can lead to major improvements and a general reduction of the cycle time while improving the heat transfer [5]. AM technologies are capable of fabricating these complex conformal cooling channels.

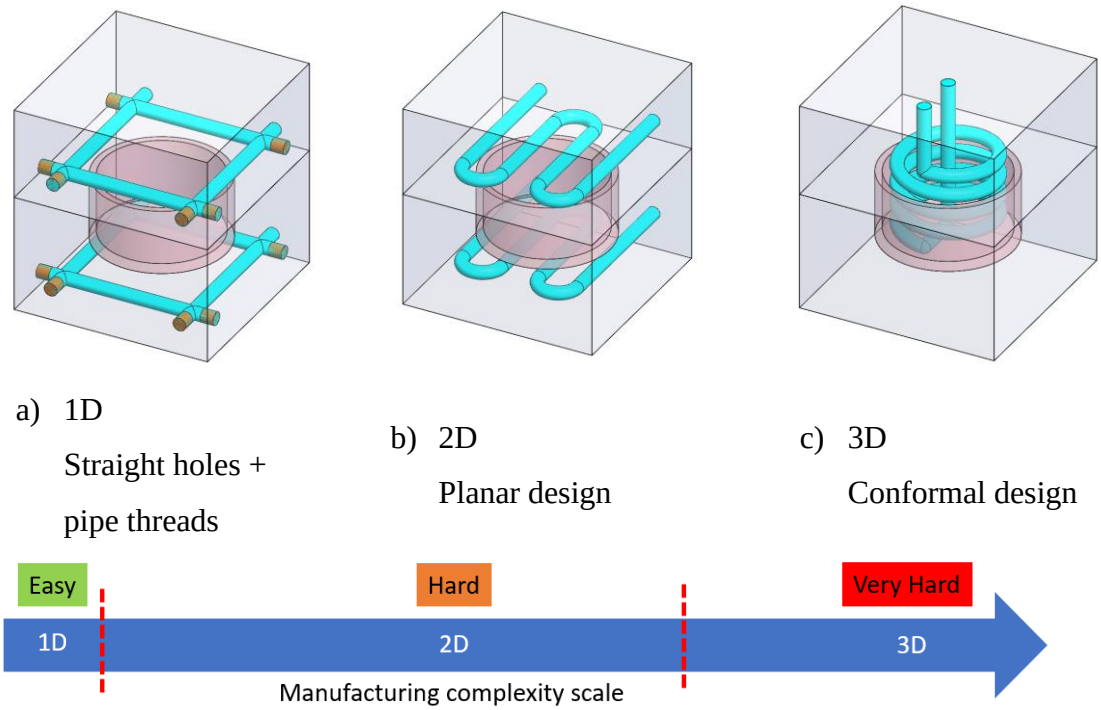

Figure 1.7 Manufacturing complexity of building internal features in a mold

Metal and plastic AM technologies are capable of fabricating highly complex geometries. However, each AM family has its advantages and disadvantages. For example, the FDM process is suitable for rapid prototyping, construction of complex geometries, and has only a few design limitations. But this process is expensive, slow, and the range of materials for the FDM process is relatively limited. As a result, an FDM technology is not an economical choice to directly build a low to medium (10-5000) batch of products. Choosing a production number and categorizing production volumes are totally scenario-dependent and there is no established number to separate low, medium, and high production. Printing one of the door handles developed in this research, had cost around 50 CAD dollars for the material and took 4 hours and 2 minutes to be fabricated (see Figure 1.8). Using FDM technologies to directly build a tool for IM is not a sensible solution due to the high temperatures and high forces involved in an IM process which will cause the FDM-built tool to fail [10].

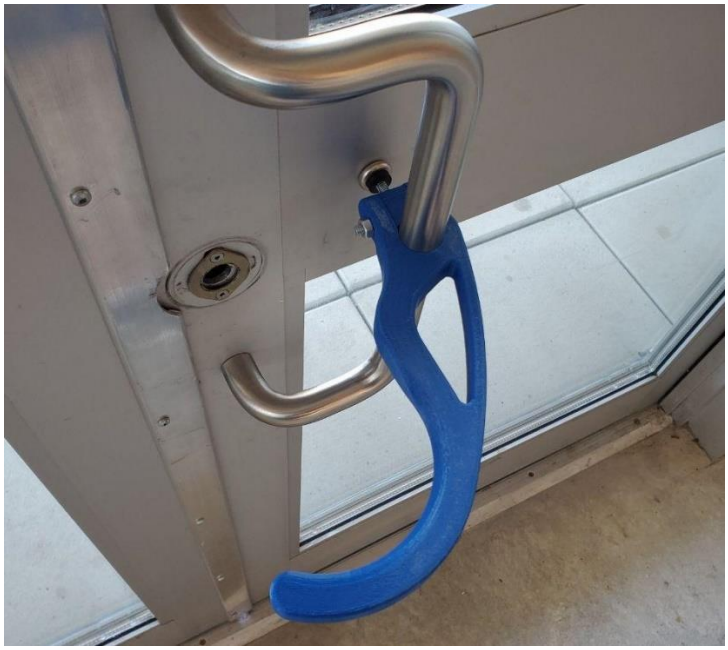

Figure 1.8 Extended door handle design built via FDM technology. Material price for this handle cost around 50 CAD

On the other hand, metal AM technologies can be used to build a tool that can fabricate thousands of a product. Additionally, internal features such as conformal cooling channels can also be built inside a mold, as it will be demonstrated in this research. As mentioned before, cooling channels play an important role in an IM process. However, using metal AM solutions to build internal features has its own limitations. As reported by Tan et al [11], the top layers of the inner wall of a channel can cause material collapse due to high overhang angles. Besides, the residual stress introduced in a metallic AM process can lead to warpage and distortion. As a result, the maximum diameter of the cooling channels that were manufacturable without support structure was limited to 8 millimeters. To increase the diameter of the channels, support structures are required inside of the channels. As illustrated in Figure 1.9, because the construction of the support structure was unavoidable, Tan et al concentrated on optimizing the support geometries.

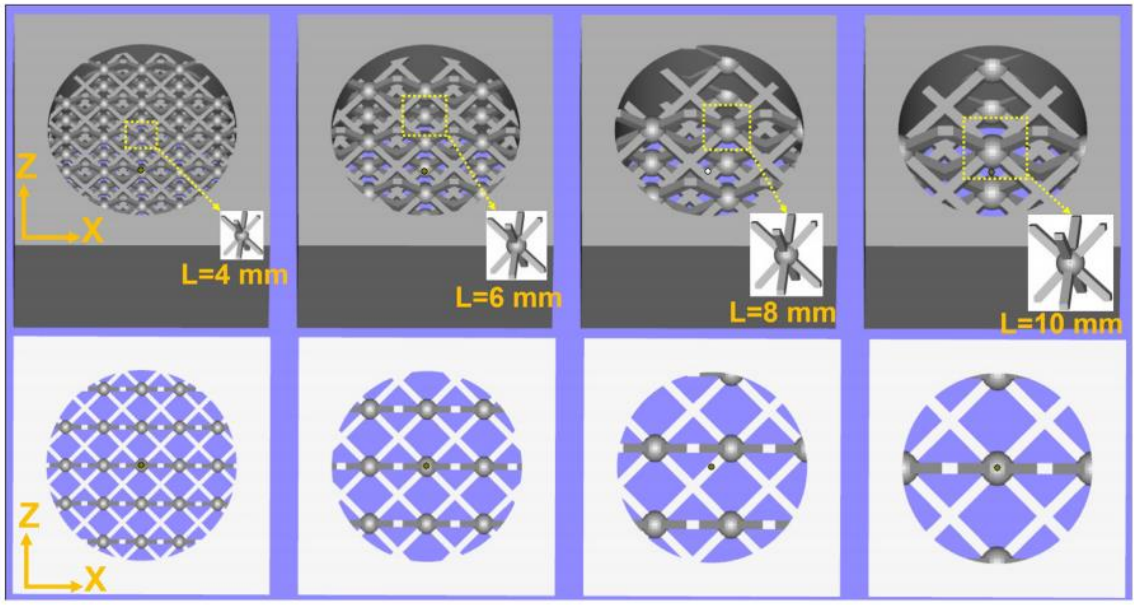

Figure 1.9 Optimization of support structures inside conformal cooling channels [11]

Another major issue in using metal AM technologies to build a tool, is that the process, raw material, and final product are very expensive. Also, the mold sets built via metallic AM, need to be post-processed and machined. As a result, conventional and metallic AM-built molds are not economically justified for low to medium production. This clearly shows the importance of a low-cost and rapid tooling solution that is suitable for low to medium production. Also, a new method needs to be developed to build complex internal channels without additional support structure on the inside, which is the objective of this thesis.

1.4 Research Objective

To fill the gap between the conventional and AM-built molds, the main objective of this thesis is to develop an alternative, significantly low-cost, and rapid tooling that requires less time to be manufactured than conventional mold making processes. This tooling solution is suitable for low to medium (10-5000) production. The injection material for this tooling limited to high-temperature plastics that have an injection temperature of less than 300 ℃. The second objective of this thesis is to investigate the possibility of constructing internal channels with no support structures. If complex internal channels are capable of being manufactured without any additional support structures, further studies can be

conducted to develop a heat model to maximize the cooling capacity, efficiency, and design an effective cooling system inside the tool.

1.5 Thesis Outline

Chapter 2 presents an overview of the FDM process, literature review of contemporary rapid tooling solutions, and shows the state of the art in manufacturing complex cooling channels. The research gaps are identified and the necessity of the work in this research is further discussed.

Chapter 3 covers the methodology that has been followed in this research. The process flow starting from designing new products, design for manufacturing (DfM), virtual validation, and experimentation will be explained. The tools, limitations, and solutions are discussed in detail. Development of the low-cost rapid tooling solution will be presented step by step and each critical design decision during this research is explained and justified.

In chapter 4, the results of each experiment are discussed. The validation of virtual studies, proof of concept, and final results are presented. The final results of this solution are analyzed, and image processing methods are used to evaluate the final product.

Chapter 5 includes the conclusions and recommended future work activities.

CHAPTER 2

LITERATURE REVIEW

2.1 Fused Deposition Modeling (FDM)

This research project employed the fused deposition modeling (FDM) material extrusion process, which has been developed by Stratasys Ltd. The developed FDM machine, Fortus 400mc, is capable of fabricating parts from conventional FDM materials such as ABS to high-performance materials such as ULTEM 9085. However, compared to an injection molding process, the materials available for an FDM machine is relatively limited.

Table 2.1 shows the mechanical properties of the material used in this research. For this research ABS M30i, ULTEM 9085 Resin, and PC-ABS were used to fabricate different components.

In an FDM process, the printing material is fed through a heated element in the shape of a filament. The material reaches a semi-molten state and is pushed through a nozzle. Beads are deposited side by side on a build platform to create a thin 2D geometry. These 2D geometries are stacked on top of each other (layer by layer) until the desired 3D geometry is created. [12]. Figure 2.1a represents a schematic of a conventional FDM process. In this research, a Fortus 400 MC (see Figure 2.1b) was used to create the prototypes as well as functional components.

Since FDM technologies are capable of fabricating components without any tooling, they are best suited for prototyping. However, due to high cost of material and high production time, using FDM to fabricate a low to medium batch of products, is not very sustainable. Figure 2.2 shows the build information of an extended J-hook which has been designed in this research. Using FDM technologies to build this component, costs more than 50 CAD dollars per piece (for the material). Considering that each J-hook takes almost 3 hours to be fully built, it would not be very sensible to choose FDM technologies as a production method.

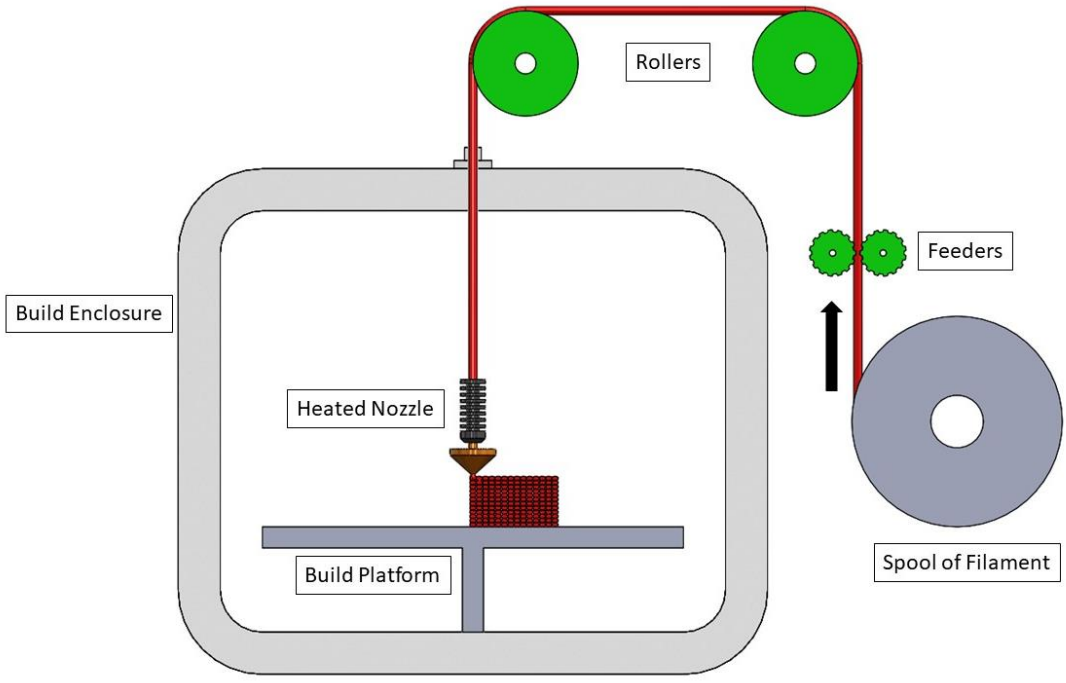

a)

b)

Figure 2.1 Fused deposition modeling process schematic(a); The Fortus 400 MC (b)

Table 2.1 Properties of FDM materials used in this research, made by Stratasys [13]

Material	Tensile Strength (Mpa)	Tensile Elongation (%)	Flexural Strength (Mpa)	Impact Toughness – IZOD notched (J/M)	Heat Deflection Temp. (℃)	Glass Transiti-on (℃)
ABS-M30	36 Mpa	4 %	61 Mpa	139 J/M	96 ℃ at 66 Psi	108 ℃
ULTEM 9085	71.7 Mpa	5.5 %	107 Mpa	94.8 J/m	176.9 ℃ at 66 Psi	177.32 ℃
PC-ABS	36 Mpa	3.01 %	No Break	240 J/m	125 ℃ at 66 Psi	105 ℃

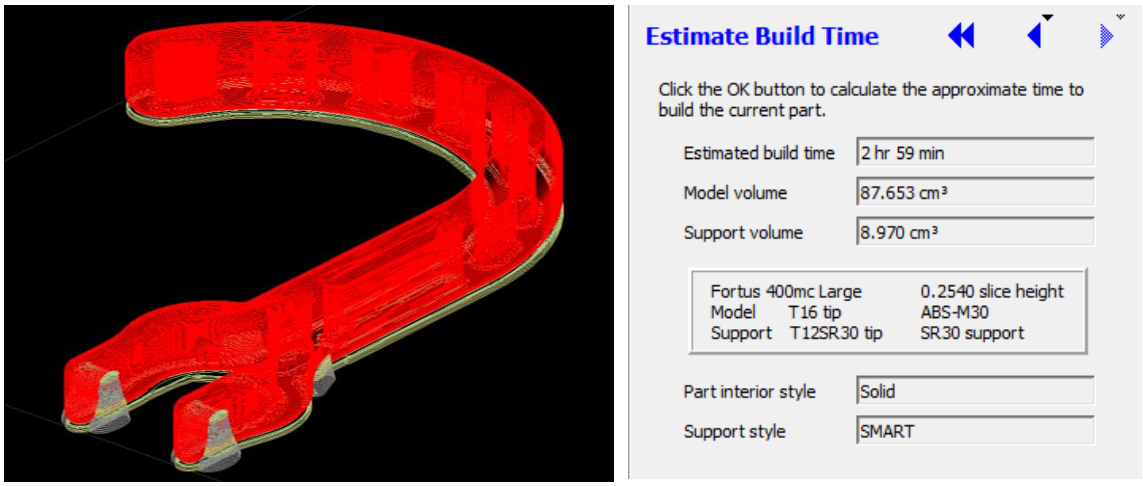

Figure 2.2 Build information of J-hook with FDM. The material piece price is almost 50 CAD

As previously explained in section 1.2, AM processes need support structures in order to build components with exceeding overhang angles. FDM processes need the same solution for building overhang features. The removal of support structure is an additional process that needs to be done after the part is finished building. This will add extra processing time to the already time-consuming printing process. To facilitate post-processing operations, Stratasys Ltd. has developed a series of soluble support materials that are dissolved when exposed to a special solvent [14]. Even if the use of soluble support is more convenient, it still adds a post-treatment step to the fabrication process. Therefore, the production time is yet again increased. As a result, it is preferable to avoid using support material while fabricating a component, especially on the inside where access can sometimes be difficult. This soluble support material is leveraged to play a key role in the developed solution to build the internal channels and mold cavities. The solution is further discussed in the research methodology section.

Considering all the process capabilities and limitations of FDM, this process will not be a suitable manufacturing solution for low to medium production runs. This will further highlight the need for a tooling solution that is built relatively fast and is significantly more cost-efficient. Using rapid tooling solutions will enable handling low production volumes and is economically more sustainable. In the next chapter, related literature on rapid tooling solutions is reviewed.

2.2 Literature Review on Rapid Tooling

Levy et al. [15] conducted a full review of rapid manufacturing and rapid tooling with layered manufacturing technologies and analyzed the prospects. Levy et al. defined rapid tooling as a tool that can make thousands of parts before wearing out. The definition of this tooling is confined to plastic injection molding applications only. They studied different AM processes and analyzed their capabilities in creating different tooling designs. They believed that rapid tooling made by AM processes can be used in a wide range of applications, from soft tooling (low/limited volume) to hard tooling (selective laser sintering- SLS tooling for up to 100,000 shots). However, they stated that the breakthrough of these technologies to make an operating tool primarily depends on the cost and productivity.

Karapatis et al. [16] stated that rapid prototyping technologies are moving toward rapid tooling. They believed the motive behind this move could be to reduce the time for placing an item on the market by reducing not only the development phase, but also the industrialization phase of the manufacturing process. They analyzed the processes and limitation of the process such as density, dimensional accuracy, surface roughness, mechanical properties, etc.

Akula et al. [17] developed a rapid tool manufacturing process called hybrid-layer manufacturing (HLM) to manufacture metallic dies and tooling. They used MIG welding process to create a near-net shape and used CNC machining to bring the design to the final finish and dimensions. The HLM process used the following numerical control programs to create the tooling:

i. Toolpath for weld deposition
ii. Toolpath for face milling every layer.
iii. Toolpath for finish milling

In their research, they reported that the overall cycle time to produce tools and dies was much faster via HLM compared to the existing technologies of the time. They indicated that the welding process did not achieve all the desired properties of the material. Besides, they reported that even though their tool had a lower quality in composition and tool life compared to other conventional tools, they believed their tool could manufacture the final product as accurately as other conventional tools.

Kalami et al. [10] designed and fabricated a low volume injection mold and followed a rapid tooling approach that was suitable for a high-temperature material. In their research, they reported that material costs are high for metallic AM technologies and plastic based AM technologies will not be suitable for a tooling solution due to thermal conductivity and material compatibility. In their studies, they used material extrusion-based AM (FDM) to create sacrificial cavity patterns. However, these patterns were not soluble and had to be removed after building the cavity. To build the mold, they used the thermally conductive Aremco 805 epoxy that has been used in this research as well.

As discussed in Section 1.1, cooling channels play an important role in tooling solutions and highly affect the economics and quality of the final product. However, fabricating

complex channels inside a tool is very difficult and highly limited by manufacturing constraints. As a result, the effectiveness of the cooling systems is reduced. In the next section, the effects and manufacturability of complex cooling channels have been reviewed.

2.3 Literature Review on Additional Cooling Channels

Sachs et al. [18] was one of the first to study the effect of cooling channels on IM quality. They investigated the effect of cooling channels on injection molding and reported that conformal cooling improves the control of mold temperature and part dimensions.

Wu et al. [19] worked on the optimization of additive manufacturing for injection molding through simulation. They realized that they could reduce the molding materials. In their research, they used spiral cooling channels and in their simulations, the core and cavity were made of stainless steel and the final piece was made of polypropylene.

Shinde et al. [20] carried out a case study on a rapid prototyping-assisted conformal cooling channel (CCC) that is used in the industry. They reported that additively manufactured conformal cooling channels might become standard procedure in injection molding. They stated that a CCC improves quality and productivity. The main focus of their research was on simulation and they indicated that more research is required for the fabrication of molds with CCC. Besides, the high cost of metallic AM molds was one of the limits of this project.

Jahan et al. [21] developed a numerical model to represent the thermal behavior of CCC in dies. Following numerical analysis, they experimentally validated their model. Their objective of their research was to produce a cylindrical plastic bottle cap. To accomplish this, they created a two-piece core-cavity die made of structural steel. Although the size of the final product was small, they reported that cooling channels with rectangular cross-sections were the most effective design.

Mazur et al. [22] studied the usage of conformal cooling channels made by selective laser sintering (SLM) AM and used H13 tool steel as the material for their experiment. As a part of their research, several physical and numerical studies were conducted to quantify SLM-manufactured H13 cooling channels. They were concerned about the porosity of parts

manufactured for injection molding. The fabrication of cooling channels with circular sections was studied and they realized stress concentration in the SLM process can lead to compromises in dimensional accuracy. To assess the stress concentration on the circular cooling channels, they conducted a numerical analysis. Finally, they experimentally evaluated the fabrication of cooling channels as lattice structures and studied the manufacturing parameters. These lattice structures were tested to evaluate the effect of lattice types and cell sizes on strength and stiffness.

Tan et al. [11] designed an injection mold in which the cooling channels were designed in a self-supporting configuration. In addition to the cooling channels, they included porous structures in the mold to improve cooling efficiency and the same AM fabrication costs. After designing the channels, they performed numerical simulation via Moldex3D to assess the cooling performance of the CCCs. After designing channels that would be built with self-supporting structures, they used laser powder bed fusion (LPBF) to build the channels to evaluate the manufacturability of the designs. Even though the writers claimed that they had made self-supporting structures, as could be seen in Figure 2.3, there are support structures inside the channels. The effects of different sizes of cooling channels were studied via simulation.

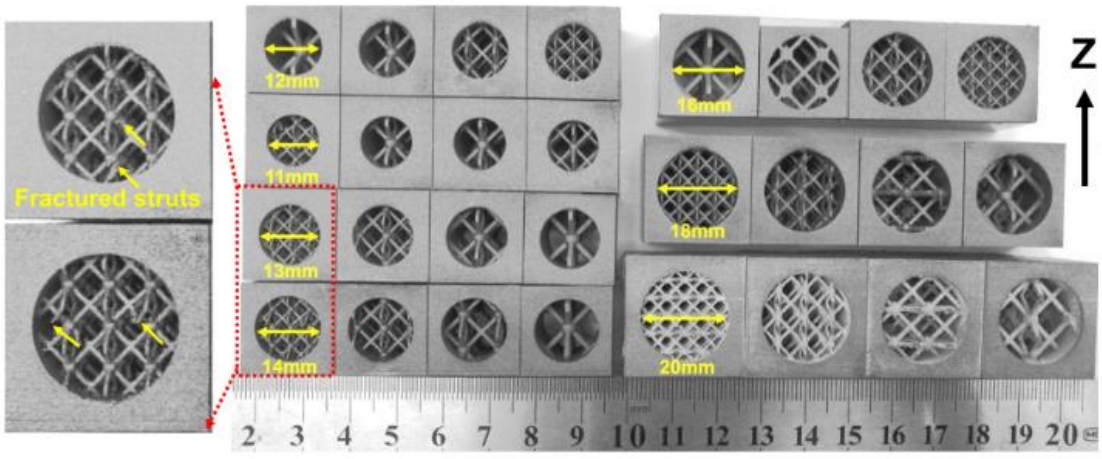

Figure 2.3 Images of manufactured channels with internal support structures by Tan et al. [11]

The literature reviewed for this research has been summarized in Table 2.2.

Table 2.2 Literature review summary

Authors	Rapid tooling	Low-cost solution	Design for manufacturing	Virtual study	Experimental study	Complete mold with internal features	Used AM technology	Comments
Tan et al. [11]				✔	✔		LPBF	Simulated the effect of cooling channels and created several cooling channels with different diameters via laser powder bed fusion (LPBF). This was not a functioning tool.
Levy et al. [15]	✔							Review on rapid tooling processes
Karapatis et al. [16]	✔							Review on rapid tooling processes
Akula et al. [17]	✔				✔		HLM	Built a rapid tooling die with the developed hybrid layered manufacturing (HLM) process
Kalami et al. [10]	✔	✔			✔		FDM	Rapid tooling of low volume of an injection mold using fused deposition modeling (FDM)

Authors	Rapid tooling	Low-cost solution	Design for manufacturing	Virtual Study	Experimental Study	Complete mold with internal features	Used AM technology	Comments
Sachs et al. [18]	✔							Review on cooling channels and their effect on quality
Wu et al. [19]				✔				Simulation of tooling with conformal cooling channels
Shinde et al. [20]	✔			✔				Simulation on tooling with conformal cooling channels. Reported expensive experimental setup
Jahan et al. [21]	✔			✔				They designed the setup to make plastic bottle cap. (small size) CCCs with rectangular cross-sections were the most effective design.
Mazur et al. [22]				✔	✔		SLM	Reported high stress concentration in cooling channels made by selective laser melting (SLM)
Pasha	✔	✔	✔	✔	✔	✔	FDM	Low-cost tooling solution with reduced manufacturing time and internal channels

According to the literature reviewed, the majority of the research has focused on costly metal additive technologies. Moreover, metallic AM technologies require support structures to build 3D internal channels. Consequently, the state of the art is primarily based on simulations, and the scope of the experimentation is limited to the construction of a section of a tool with an internal feature. None of the reviewed literature built a complete rapid tool that is low-cost and at the same time contains internal features. The majority of the researchers reported that the high cost of metallic AM processes was a limiting factor in their studies. As a part of this research, design for manufacturing (DfM) concepts have been applied to the product design, which are very limited or missing from the reviewed literature. As reported by Jahan et al. [21] rectangular cooling channels are the most effective but they are hard to be manufactured without adding internal support structures. As a result, the developed tooling solution will have rectangular channels that require no support structure on the inside. This can further strengthen the contributions and novelty of this research. The state of the art demonstrates a lack of research for a low-cost tooling solution at the same time has the capability of building complex and precise internal channels. This solution will have a fraction of the cost of metallic AM technologies and will require a shorter time to be built. The process flow for building this low-cost rapid tooling solution with internal channels will be further discussed in the methodology section.

The methodology and process flow for this work is further discuss in the next section.

CHAPTER 3

METHODOLOGY

To achieve the objective of this research related to the development of a low-cost rapid tooling solution, the fingerless door handle (J-hook) was selected. The reason behind this selection is due to complex geometries and unique challenges in its design. This component was designed with relatively thick wall designs, and if this solution was deemed suitable for this complex geometry, it will be suitable for other products with less complex geometries. Figure 3.1 shows the methodology used in this research. To further highlight the importance of each step, a color-code system was used. As the shades of green get darker in Figure 3.1, the more important the steps become. The materials used in this study are illustrated in Figure 3.2.

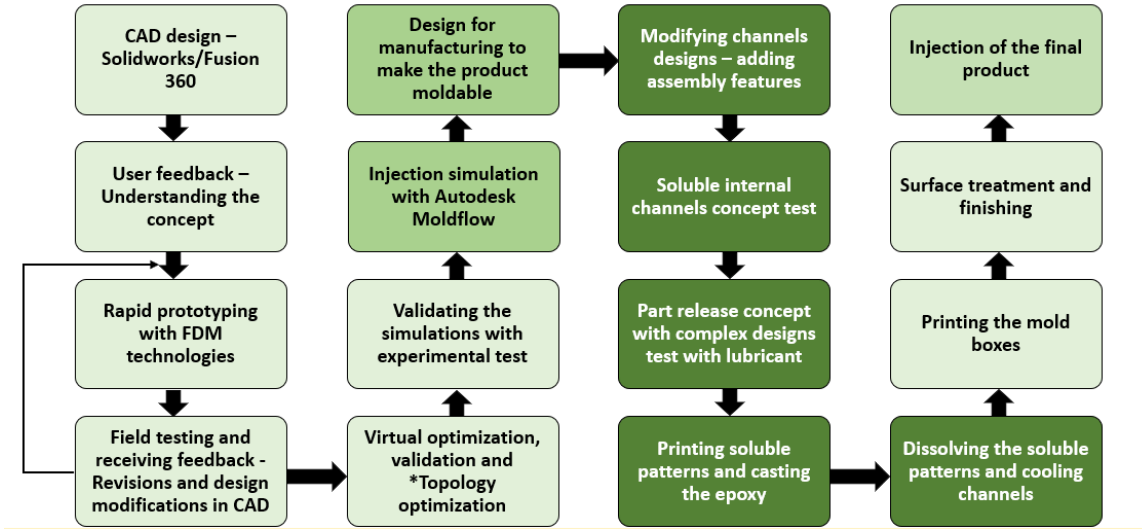

Figure 3.1 Summary of the methodology in this research

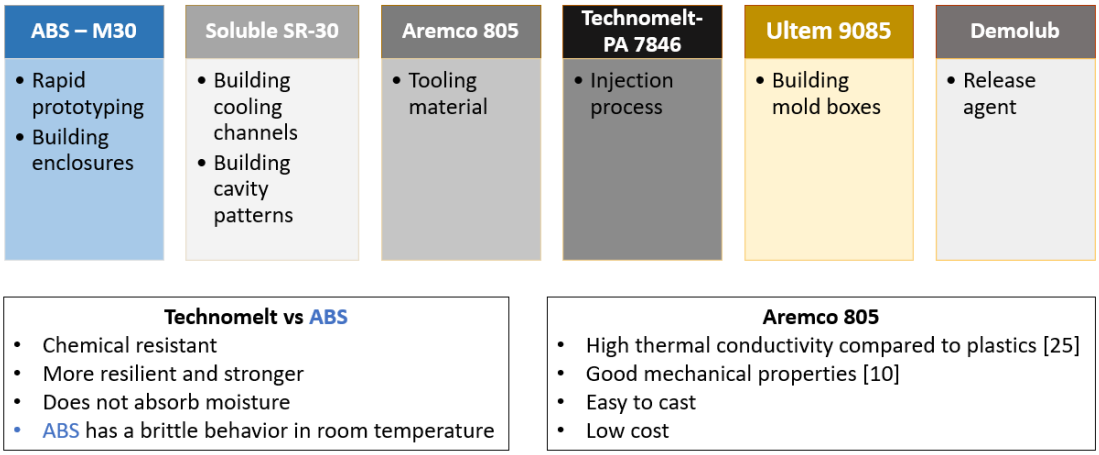

Figure 3.2 Material selection for this research

3.1 CAD Design and Product Development

Prior to this research, several personal protective equipment was designed and developed by the COVID-19 engineering research team University of Windsor. The developed products were:

- Adaptable face shield
- Finger-less door handles
- Face mask with swappable filters
- Touch-free glove remover.

Figure 3.3 shows the developed PPE by Uwindsor COVID team. The build information of these products using FDM technologies is demonstrated in Table 3.1.

Figure 3.3 The developed products including face shield, fingerless door handle, face mask and glover remover

Table 3.1 Build information of the developed PPE by FDM technology

Product	Build time	Material used
Face shields	2 hours (120 mins)	35 cm^3
Door handle	4 hours 33 mins (292 mins)	205 cm^3
Face mask	6 hours 27 mins (387 mins)	49 cm^3
Glove remover	4 hours 33 mins (273 mins)	139 cm^3

To develop a tooling solution, one of the products (shown in Figure 3.4) was selected and modified to make it suitable for a tooling process. The door handle was selected due to its complex geometry and relatively thick-wall design. This door handle was designed using Solidworks.

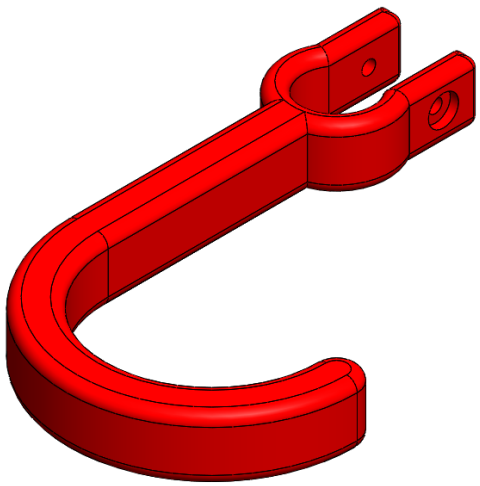

Figure 3.4 CAD design of the first fingerless door handle called “J-hook”

This handle had a circular section at the end that would fit around any circular door handle. By using a simple nut and screw the handle is fixed on any vertical bar. Once the CAD design was finished, it had to be prototyped and tested. Next, the first prototype was 3D-printed via Fortus 400MC in ABS. Figure 3.5 shows the installation and field test of the first design.

Figure 3.5 First version of door handle J-hook

To improve user experience and comfort, the fillets on the edges of the handle needed to be increased. The small area of contact provided an increased pressure to the user's hand. In the second version, a bigger fillet was added, and the contact surface created a continuous arc that increased the contact area and as a result, reduced hand pressure. The overall thickness of the part was reduced to 18 mm and the excessive material was removed from the initial design. To make this product suitable for an injection molding process, strategic ribs had to be added in the middle of the handle. These features would create a relatively constant wall-thickness so that it would not have inconsistent wall geometries during the injection process. Figure 3.6 shows the difference between version 1 and version 2 of the J-hook.

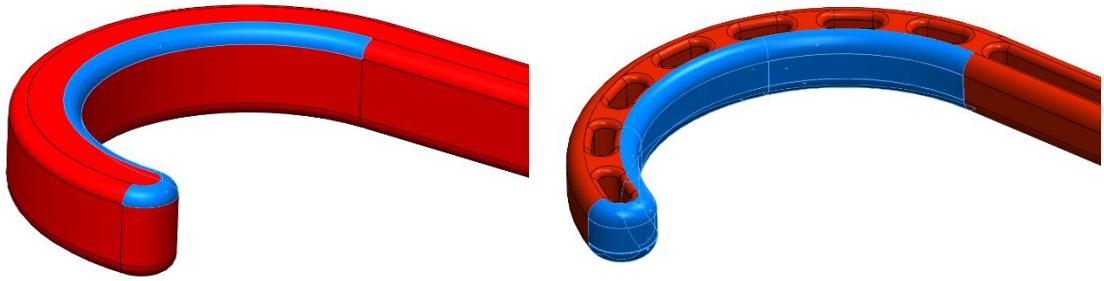

Figure 3.6 Difference between the first version and second version of the J-hook (contact area highlighted in blue.)

Next, finite element analysis (FEA) was conducted on the second version to make sure that the new design is capable of withstanding applied forces. FEA is a method to achieve numerical solutions for an engineering problem that might be complex or sometimes near impossible to be solved analytically. Since FEA studies are conducted in a virtual environment, the results need be validated in real world. In other words, the studies are applied on a geometrical model and the simulation is done on a mathematical model. Mathematical models are idealized and geometry, material properties, loads, and boundary conditions are simplified. To conduct an FEA analysis, initially, the CAD model needs to be converted into discrete elements (a mesh). The model is converted into a mesh of finite elements and each element is defined by numbering. The second step is to determine matrices that resemble the behavior of each element. Next step is to combine all the matrices into a large matrix equation and by solving this equation, the values of field quantities at the nodes are determined. For example, when such a study is conducted on a mechanical problem, stresses and displacement are the parameters of interest. These numbers are calculated after solving the main equation. Finally, the results need to be checked to make sure that they are consistent with the physics of the problem. To achieve this, the post-process function of FEA shows the results graphically [23].

To run the FEA analysis, CATIA V5 was utilized. The pulling forces required to open several doors were measured and the maximum pulling force was calculated (average 70 N). To make the simulation more representative to the real use of the handle, a vertical pushing force was added to the handle. Figure 3.7 demonstrates the application of the forces and restrains on the handle.

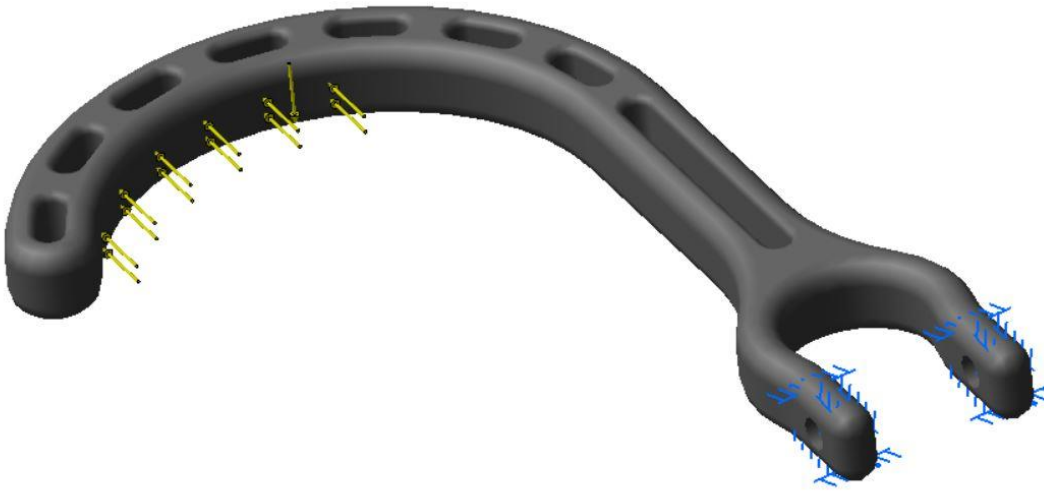

Figure 3.7 The model used for FEA simulation of second version J-hook

The material in all cases was assumed to be linear and elastic with the Young's modulus E = 2.18 GPa, and Poisson's ratio υ = 0.38. The material density is taken to be ρ = 1200 Kg/m^3 .

The part was under a distributed horizontal load of magnitude $|F_H| = 70\ N$ which is applied to the inside surface of the curvature section of the J-hook and a downward distributed vertical load of $|F_V| = 50\ N$ that is applied to the top surface of the curvature section of the J-hook. The part was meshed with 1 mm Parabolic Octree Tetrahedron solid mesh as shown in Figure 3.8. This mesh size was chosen by conducting a mesh convergence study. The reason to conduct a mesh convergence study is that for the results to be accurate, we need to demonstrate that the FEA results converge to a solution and are independent of the mesh size. [24]

Figure 3.8 The discretized mesh and the magnified view of the version 2 FEA model

As the used material behaves more brittle than ductile at failure mode at room temperature, the simulated maximum principal stress is plotted in Figure 3.9. The maximum principal stress result is equal to 29.2 MPa. However, the tensile strength is equal to 31 MPa. Therefore, the part will be able to withstand the applied forces based on the FEA simulation result.

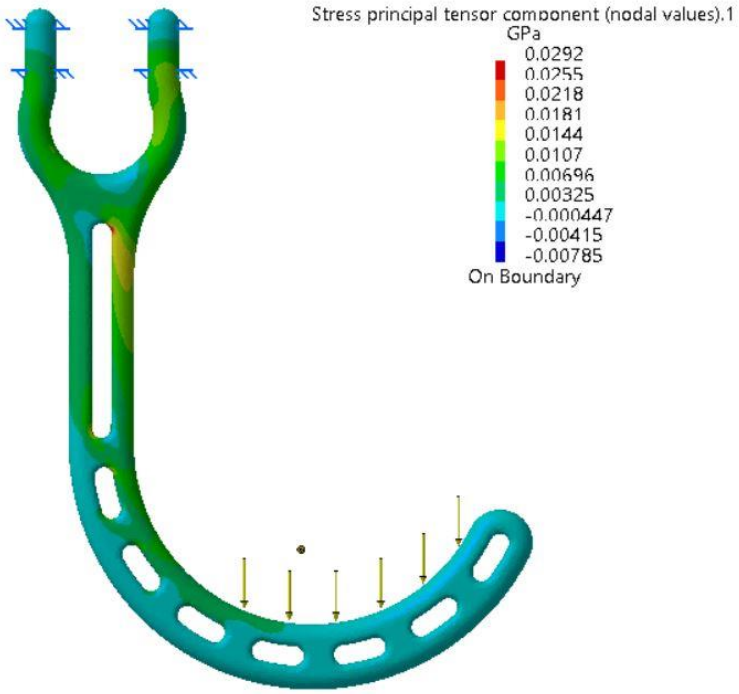

Figure 3.9 The maximum principal stress component plot for the second version J-hook FEA model

The FEA results were validated by an experimental study. For the validation process, several weights were hung off the handle to see whether the handle would yield or not. Figure 3.10 shows the setup of the weights. Each weight was hung for 60 seconds and the door was opened while under loading. Table 3.2 shows the weights and their corresponding forces.

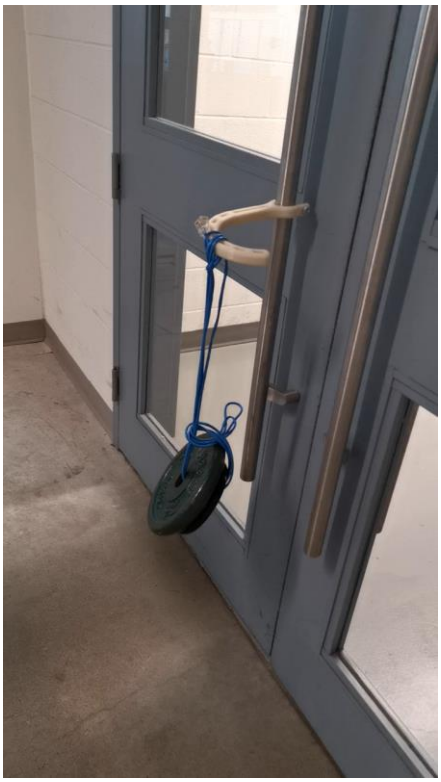

Figure 3.10 Experimental setup to validate virtual studies

Table 3.2 Weights and their corresponding vertical force

Weight (lb.)	**Corresponding vertical Force (N)**
12	57
15.5	69.5
17.5	79
20.5	91.7

3.2 Design for Manufacturing (DfM) and Virtual Validation

3.2.1 Injection Molding Simulation in Autodesk Moldflow

Once the design changes were applied to the first version, the second version J-hook was imported into Autodesk Moldflow for injection simulation. The injection temperature (200 ℃), initial mold temperature (18 ℃), and material properties were selected (Technomelt-PA 7846). The properties of Technomelt-PA 7846 are shown in Table 3.3.

Table 3.3 Material properties of Technomelt-PA 7846 [10]

Mechanical property	**Value**
Density, g/cm³	0.98
Softening point °C ASTM E28 (in glycerine)	170 - 180
Melting Viscosity at 210 °C, mPas	6,500
Melting Viscosity at 220 °C, mPas	4,500
Melting Viscosity at 225 °C, mPas	3,000-5,500
Melting Viscosity at 230 °C, mPas ASTN D 3236 (RVT, spindle 27)	3,000
Yield Strength, N/mm ISO 527 Specimen no. 5, cross-head speed: 50 mm/min	5.0
Break Strength, N/mm ISO 527 Specimen no. 5, cross-head speed: 50 mm/min	9.0
Glass Transition, °C	-30
Working Temperature, °C	-40 to 130
Softening point, °C	170 to 180

Once the simulation was conducted, the neck area of the handle which had a relatively thicker geometry compared to other sections of the J-hook, was identified as a region with potential quality issues. As mentioned before, the varying wall thickness can cause

warpage, sink marks, and shrinkage inside the part. Figure 3.11 shows the results of the injection simulation for the second version. To solve this issue, gussets needed to be used to maintain a more uniform wall thickness. As a result, several design adjustments were also required to improve the quality predictions and finalize the design for injection molding.

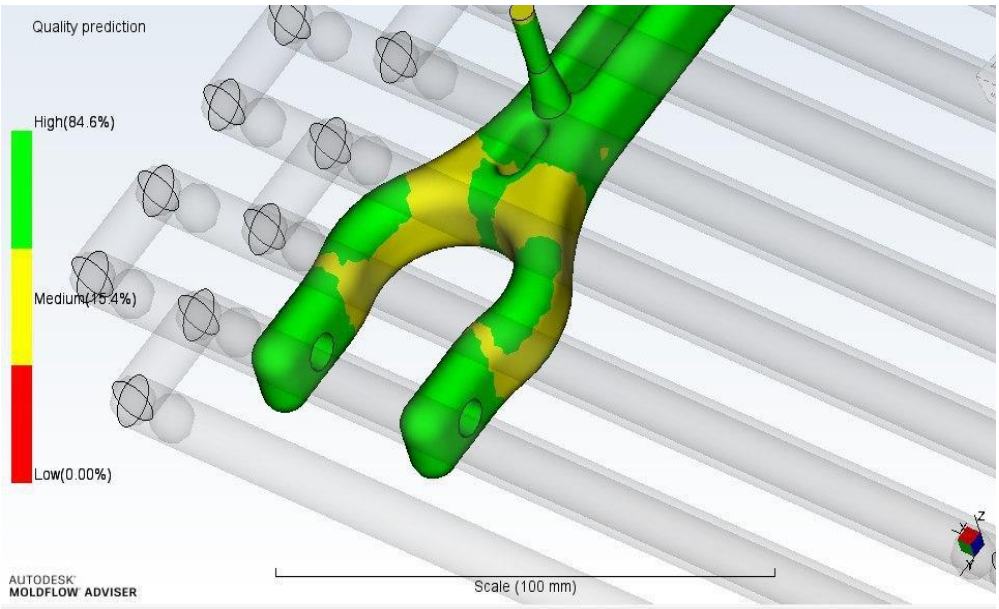

Figure 3.11 Quality prediction of the second version of the J-hook inside Autodesk Moldflow

3.2.2 Design for Manufacturing and Virtual Studies

To reduce the material in the neck area of the J-hook, the design of the part was once again modified to make the product more suitable for the injection molding process. The "rib design" approach was used to create a gusset in the neck area to maintain a more constant wall-thickness. In addition to the gussets, draft angles were needed to improve part release once the injection process is finished. At the same time, a feeding system had to be incorporated to ensure that the material would flow inside the part and can reach both ends of the J-hook at the same time. For this design, a direct sprue was selected. Figure 3.12 shows the design features that were added to the third version of the J-hook.

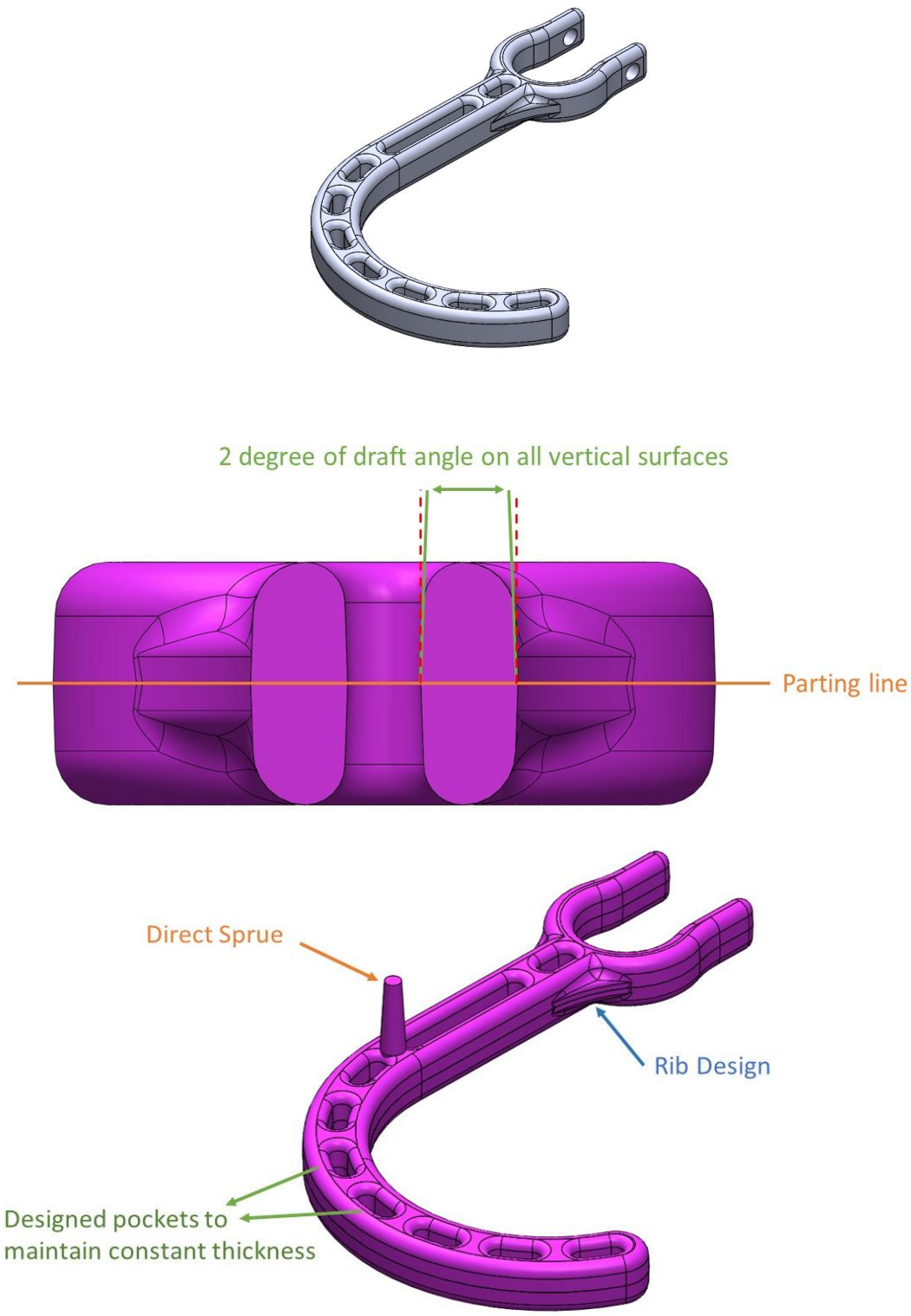

Figure 3.12 Design for manufacturing features in the third version of "J-hook"

The same injection molding process setup was used to simulate the injection in the third version. As can be seen in Figure 3.13, the questionable area has been removed and the software estimated that 96.5% of the total volume of version 3 would maintain high quality during injection.

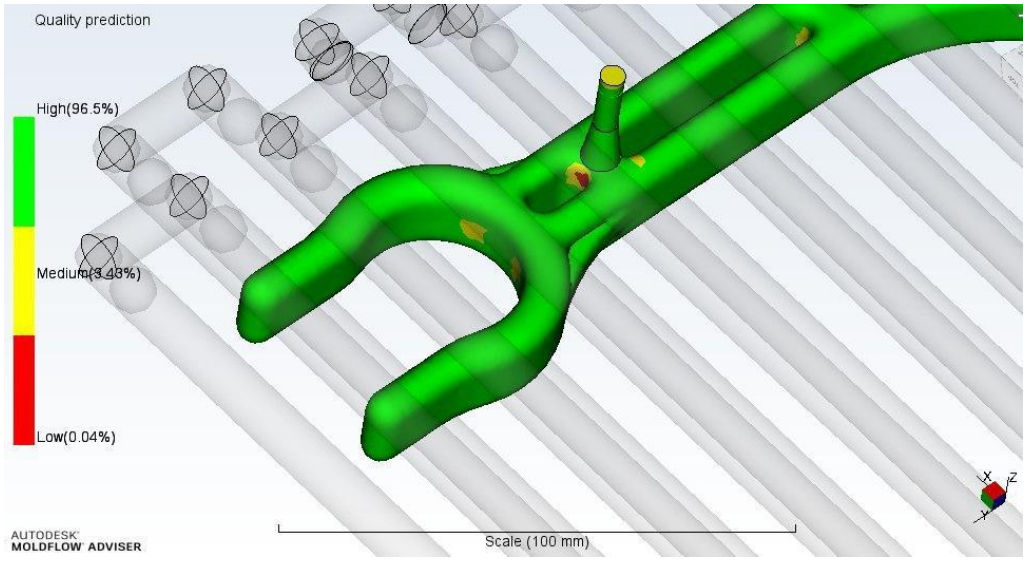

Figure 3.13 Improved prediction of the quality in version e after injection in Autodesk Moldflow simulation

Once the injection molding simulations were improved, it was necessary to conduct another FEA study for the third version of the J-hook. This FEA study is to ensure that the added design features would not introduce any stress concentration areas and affect the performance of the J-hook. So, the same ($|F_H| = 70$ N , $|F_V| = 50$ N) forces and restraints were applied to the third version as shown in Figure 3.14.

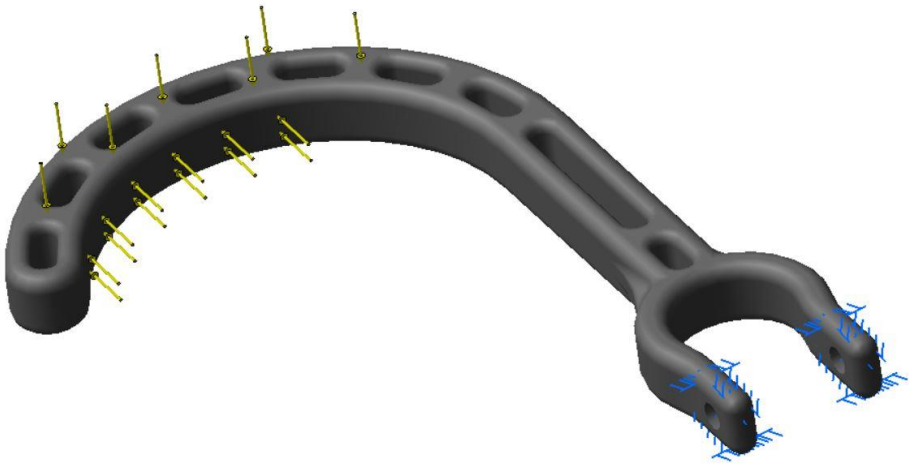

Figure 3.14 The model used for FEA simulation of third version

The model was meshed with 1 mm Parabolic Octree Tetrahedron solid mesh. A smaller local mesh size is used in the critical areas. Hence, a local mesh size of 0.25 mm was applied for the added gussets and a magnified view of the local mesh at the inside gusset is displayed in Figure 3.15. This is to clarify the differences between the adjacent element sizes. These values are chosen based on a mesh convergence study.

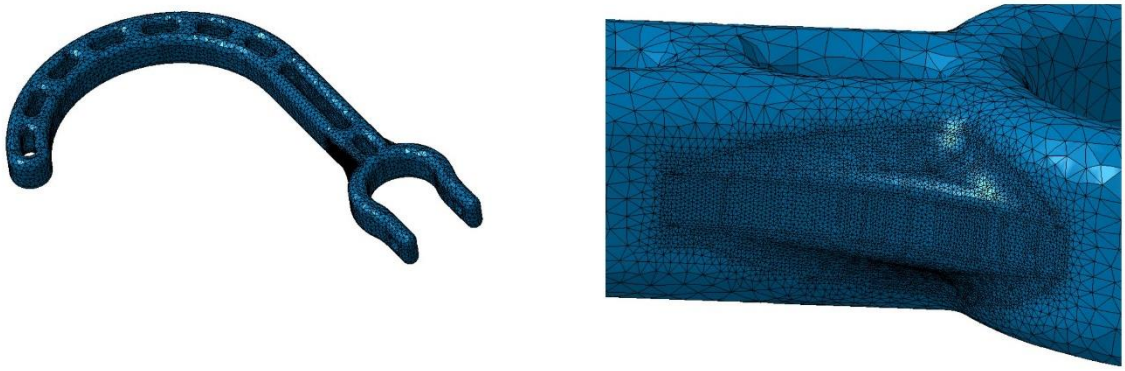

Figure 3.15 The discretized mesh and the magnified view of the local mesh of the third version FEA model

The simulated maximum principal stress is plotted in Figure 3.16 The maximum principal stress has increased to 30.9 MPa. Although the maximum principal stress has been increased by 5.82% due to design changes, the result is still satisfactory as the material

tensile strength is equal to 31 MPa. One can note that the forces applied are also considered higher than a common force applied to the J-hook by the end user. It is important to note that Technomelt PA 7846 is a stronger and more resilient material compared to ABS [25].

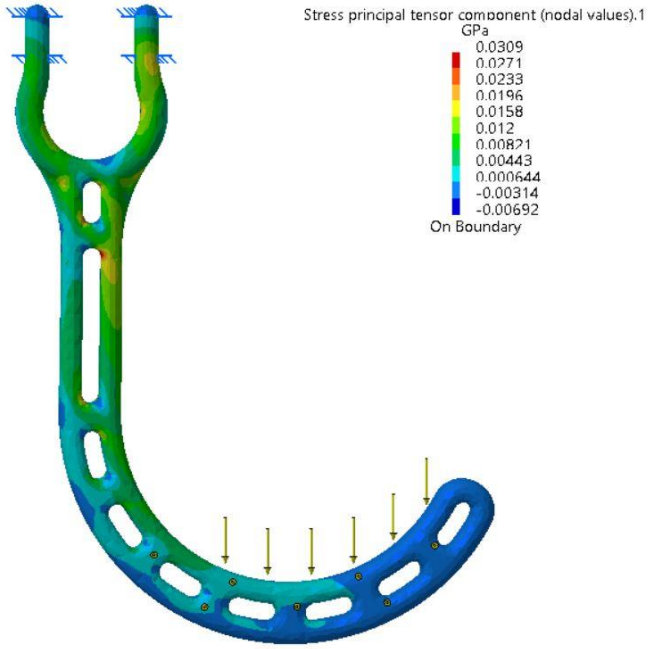

Figure 3.16 The maximum principal stress component plot for the third version of FEA model

3.3 Mold Design and Fabrication

3.3.1 Effect of Additional Cooling Channels

To evaluate the effect of adding cooling features to a mold, a simple virtual study was conducted. Thus, the same injection setup was designed in Moldflow and was simulated with and without cooling effects. In the first simulation, the cooling features were deactivated, and in the second run, the cooling features were activated. Figure 3.17 shows that additional cooling channels might have some positive effect on the ejection time, reduce the cooling cycle, and maintain a more uniform cooling. However, further research is required to validate and improve the cooling effect. This effect will be studied in detail as a future work of this research.

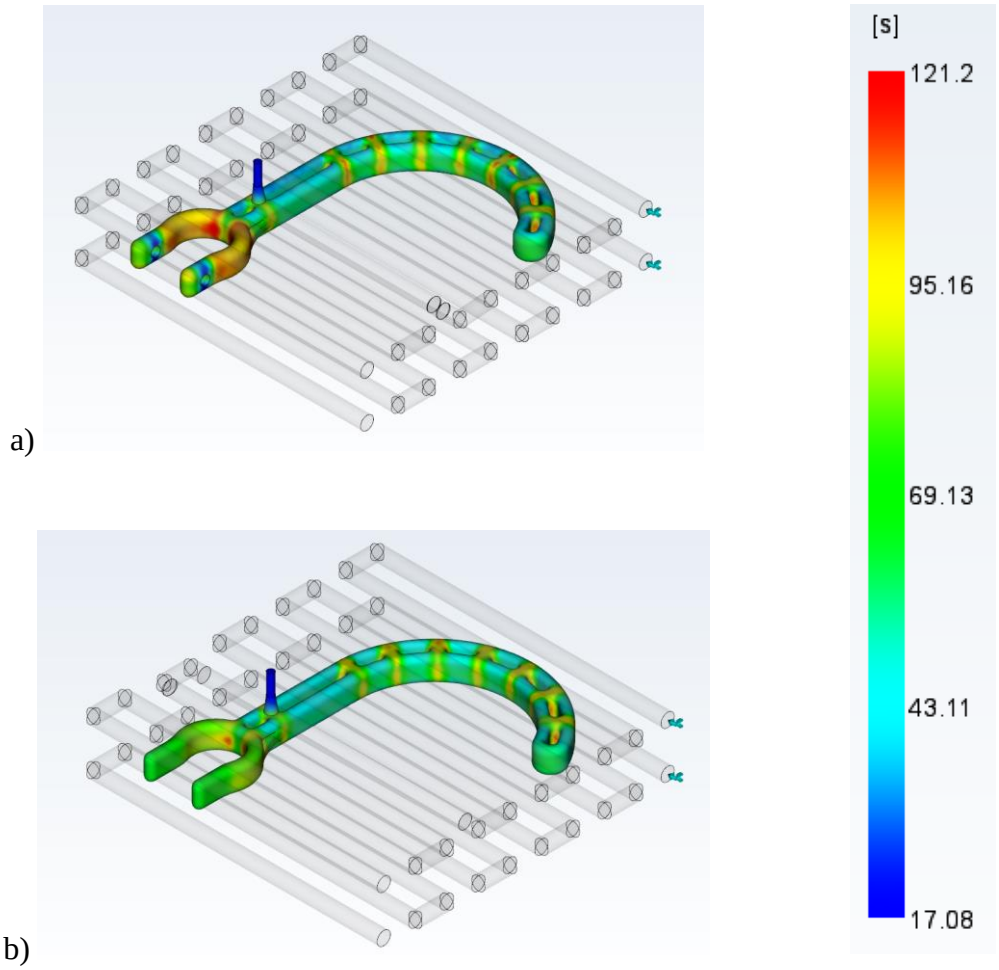

Figure 3.17 Preliminary study of cooling channels. a) cooling is deactivated b) cooling is activated. The time to eject graph has been demonstrated on the side

3.3.2 Concept Validation Strategies

With FDM technologies being too expensive and time-consuming, to build the J-hook with a fraction of the cost and with significantly lower production time, a new and novel tooling solution was designed and developed. Epoxy Aremco 805 was chosen as the material of choice to build the molds. Material properties of Aremco 805 are given in Table 3.4. The main reasons to choose Aremco 805 were that it was a heat and thermal conductor (better heat transfer characteristics compared to plastics), cured relatively quickly, and had good physical and mechanical properties to maintain injection molding temperature and

pressures. All these properties made Aremco 805 a suitable material for a low to medium volume tooling operation [26].

Table 3.4 Material properties of Aremco Bond – 805 epoxy [26]

Material	**Mix Ratio by Weight**	**Mixed Viscosity @ 25℃ (cps)**	**Temperature Resistance (℃)**	**CTE (Microns/m °C)**	**Thermal Conductivity ($W/(m^2.\frac{K}{m})$)**	**Tensile strength (MPa)**	**Flexural Strength (MPa)**
Aremco Bond - 805 epoxy	100:12	11,000	300	45	1.80	12.4	106.9

To assess the possibility of adding internal features, a special soluble SR-30 [14] was embedded inside the epoxy. When the epoxy was fully cured, it was be placed inside the support removal tank. Once the embedded support material is exposed to the support removal solution, it will be removed, and a channel would be created inside the epoxy mold. To test the validity of this idea, two experiments were designed to achieve the following goals:

i. Testing the manufacturability of internal features
ii. Testing part release – testing soluble patterns and ejection of the part.

i. Internal Features Test Piece

To create the internal features, a boundary box is built via FDM out of ABS-M30. This box would work as an enclosure to hold the cast epoxy. Then a spline channel is printed out of soluble support material. Once the spline channel is placed inside the enclosure, epoxy is to be poured inside the mold. After 24 hours, the epoxy is cured, and the part is then to be placed into the support removal tank. When the support material is dissolved, a clean

internal channel will be created inside the epoxy mold. Figure 3.18 shows the CAD design of this experiment. The result of this test is discussed in the results and discussion chapter.

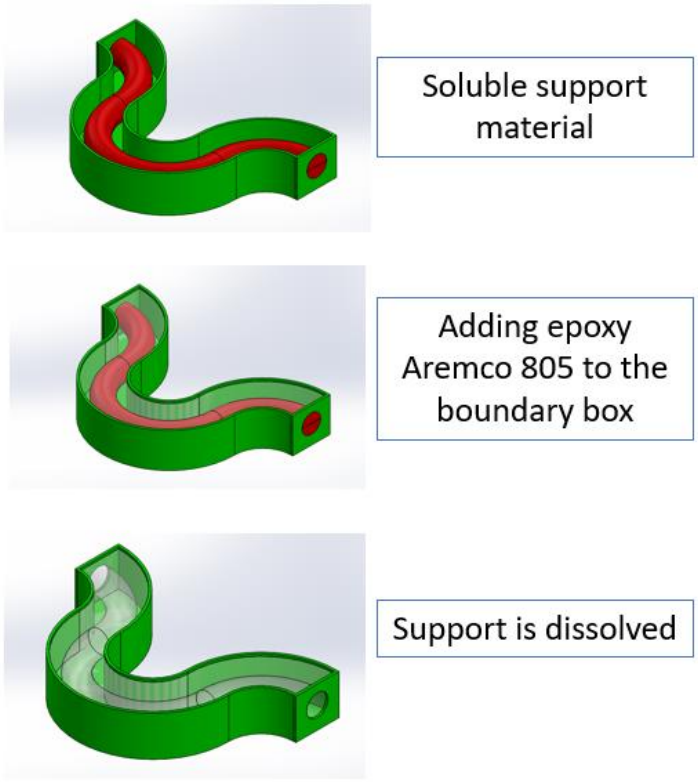

Figure 3.18 CAD design of the internal features experiment – the red section represents the soluble support material, and the green section is the ABS-M30 enclosure

ii. Part Ejection Test

Since no design guidelines exist for an epoxy-based injection mold and to ensure that the part can be released conveniently after injection, a section of the mold is created to test the draft angles and address any potential design issues. Figure 3.19 shows the CAD design of this ejection test.

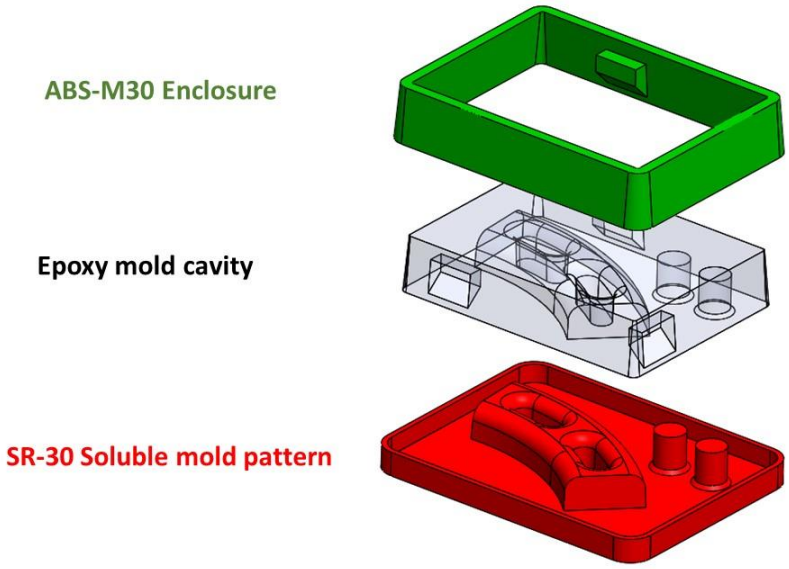

Figure 3.19 Exploded view of the release test

To create the cavity, the cavity is printed with the same soluble support (SR-30) and the enclosure around it is built via ABS-M30. The combination of these two parts creates a pocket for the epoxy to be poured in. After the epoxy is cured, it is to be placed into the support removal tank and after the solution of the support material, the cavity is formed. Once the cavity is ready, a layer of Silicone-free mold release agent (Demolub) [27] is applied to the cavity surface. Finally, molten Technomelt-PA 7846 is to be poured into the mold cavity. The results of this experiment are discussed in the results and discussion chapter.

By doing these proof of concept tests, the main concept of rapid tooling with special cooling channels are to be validated. For the next step, the main mold is to be built in full size.

3.3.3 Final Mold Manufacturing

i. Modifying the Design of the Internal Channels

According to the existing literature, conformal cooling channels with rectangular cross-sections would provide a better cooling effect compared to circular cooling channels [21]. Since as a secondary objective of this research we are evaluating the possibility of manufacturing internal features, an internal channel with rectangular cross-section was designed. Rectangular channels are very hard to be built. Conventional machining solutions are incapable of drilling rectangular holes and additively-manufactured channels would require support material on the inside. However, if these channels were designed to be printed as a single component, they would require support material on the inside as well. Figure 3.20 shows the CAD design and also the support material generated by the Insight® slicer software.

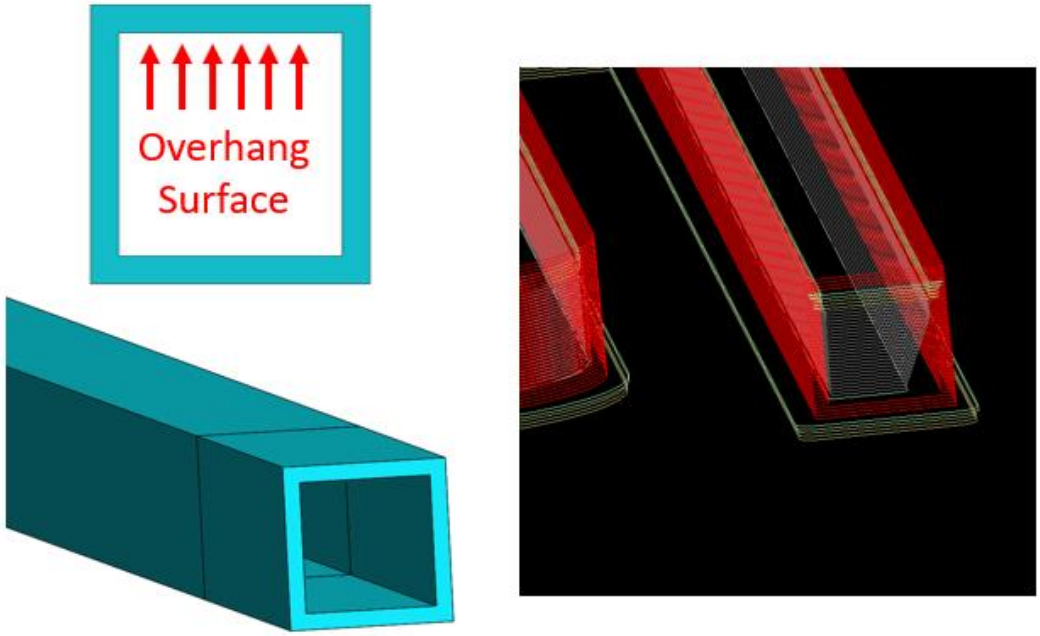

Figure 3.20 Generation of support material for the overhang surfaces on top

To address this problem, the rectangular channels were split into two different sections to avoid generating support material. To facilitate the assembly, additional features were added to the top section. Figure 3.21 shows the new split design and lack of support material in the slicer software, Insight®.

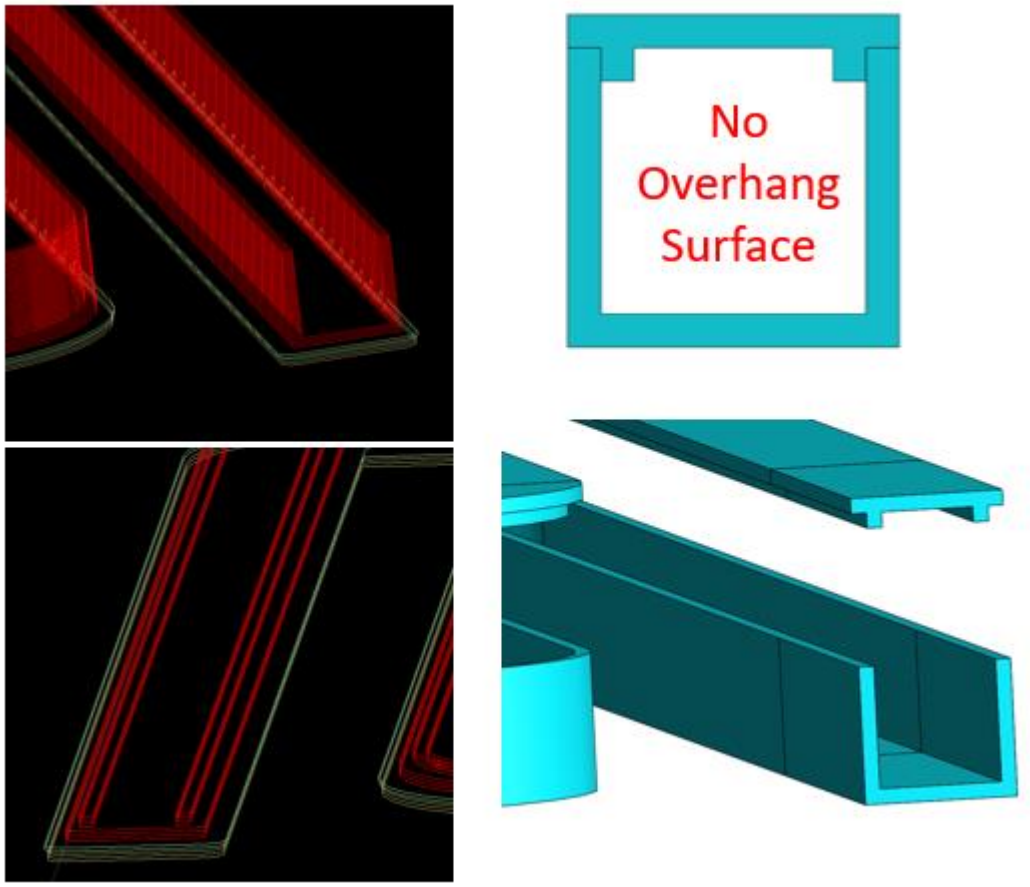

Figure 3.21 Split design of the soluble internal features without additional support structure

ii. Final Mold Design with Internal Features

To build a mold with epoxy Aremco 805, a boundary box and a soluble pattern were designed. The soluble pattern was made from soluble support (SR-30). This pattern contained the cavity with drafts and the sprue for the feeding system. Figure 3.22 shows an exploded view of the mold assembly.

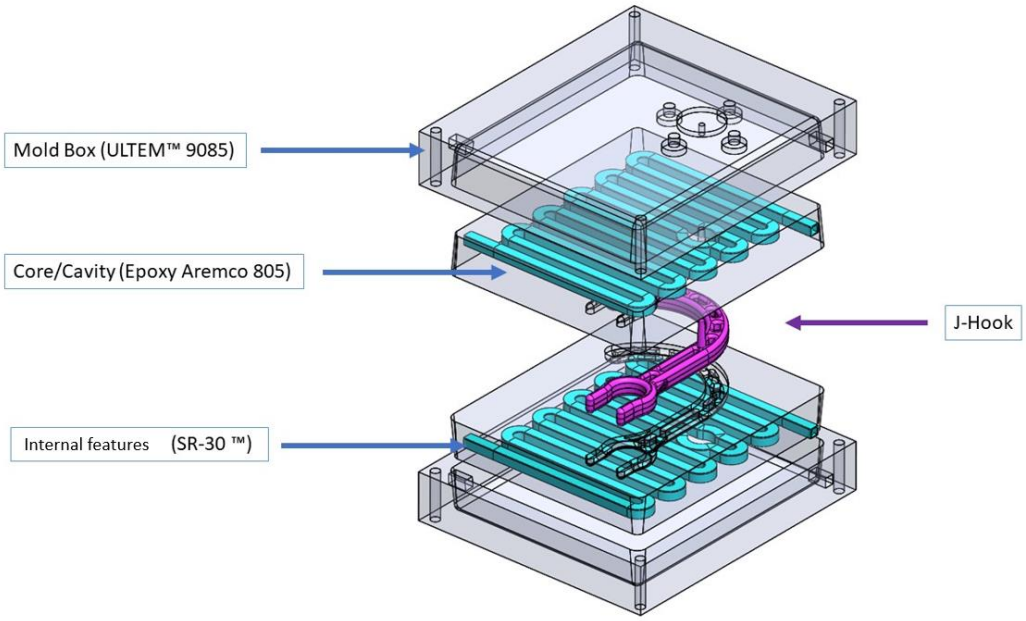

Figure 3.22 Exploded view of the mold assembly

Figure 3.23 shows the exploded view of each mold cavity.

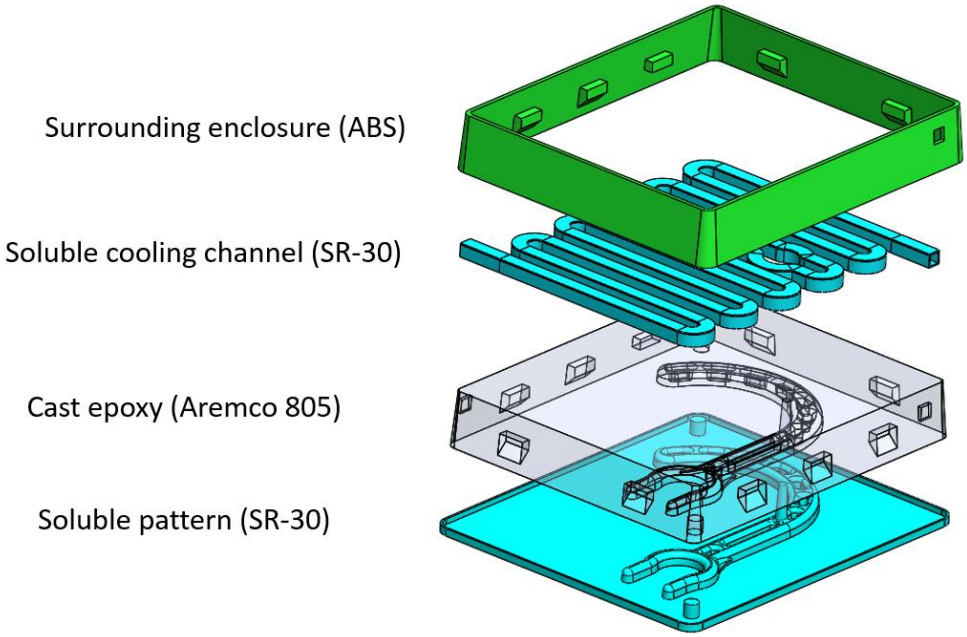

Figure 3.23 Exploded view of the mold cavities

iii. Manufacturing Mold Components

To build the cavity blocks, a soluble pattern from each side of the J-hook was built via FDM. An ABS-M30 enclosure was placed on the soluble pattern to make sure that epoxy would not leak after casting. To further seal the edges, glazing compound [28] was applied on the edges. Afterward, the soluble internal features were placed in their designated locations and two sets of stands were printed out of ABS to make sure that the distance of these channels to the cavity surface is constant (10mm) throughout the mold. Once the assembly was completed, the epoxy was cast into the mold enclosure. Figure 3.24 shows the steps and the final cast.

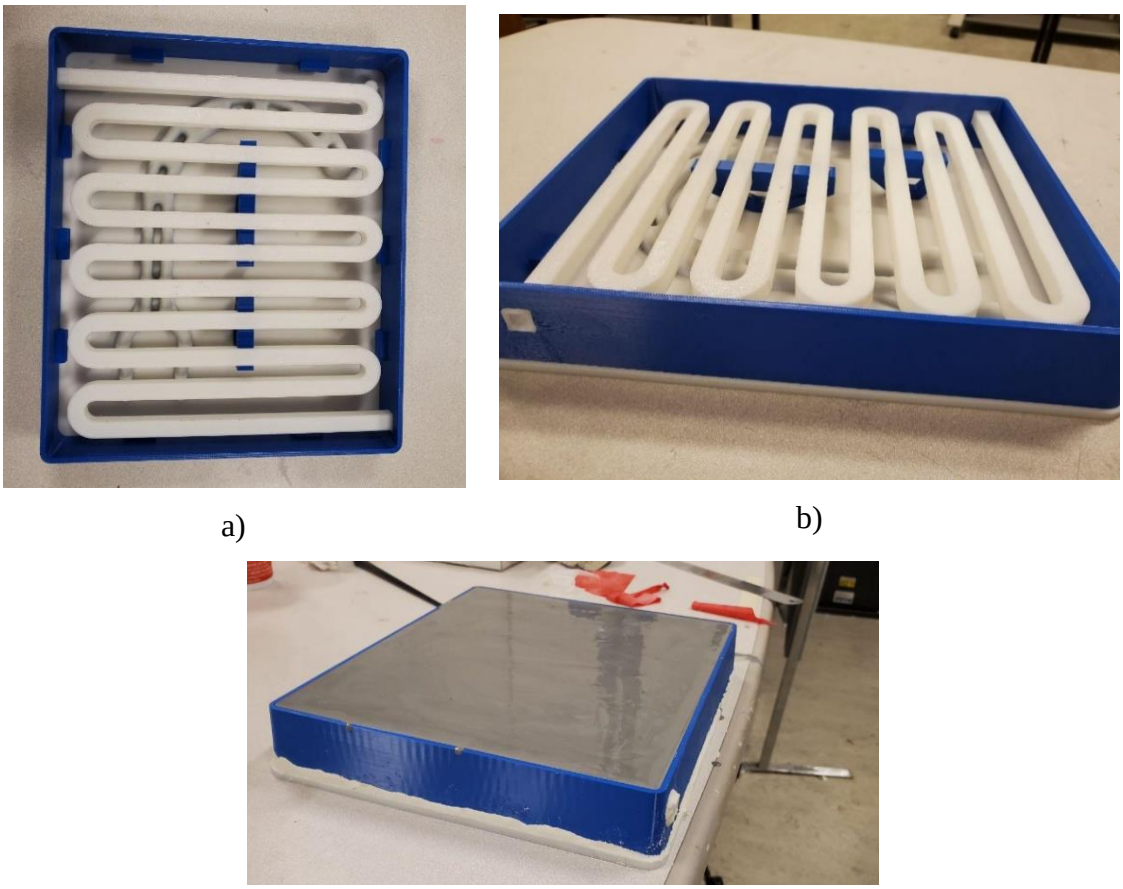

a) b)

c)

Figure 3.24 The top view of the components including cooling channels and cavity pattern (a); Side view of the mold including the stands made of ABS (b); Final step as the epoxy was cast (c)

After casting the epoxy, the part was set aside for 24 hours so that Aremco 805 would be fully cured. The same process was done at the same time to build the other side of the mold. The other section contained the sprue which was connected to the cavity and was made with the same soluble SR-30. Since the bulk of supporting material around the sprue was not enough, a block of ABS was printed to increase the strength of the material around the sprue.

Figure 3.25 shows the configuration of the top cavity.

Figure 3.25 Configuration of the top cavity prior to casting epoxy

Once the epoxy was cured, the parts were then transferred to the support removing tank and were submerged for 48 hours to remove the soluble SR-30. Once SR-30 is exposed to the support removing solution, it changes to a gummy texture that is a little sticky. To make sure that all the support material was removed, the parts were cleaned every 7 to 8 hours to enhance the solution process. Table 3.5 shows the manufacturing time to build this low-cost solution. The results are presented in depth in the results and discussion chapter.

Table 3.5 Build time information on manufacturing the low-cost tooling set-up

Process	Time
Printing the soluble top Pattern (SR-30)	3 hr 31 min (211 Min)
Printing the soluble bottom pattern (SR-30)	3 hr 50 min (230 Min)
Printing two surrounding enclosures (ABS)	12 hr 00 min (720 Min)
Printing two internal soluble patterns (SR-30)	4 hr 52 min (292 min)
* Epoxy casting and cure time (both made at the same time)	24 hr (1440 min)
Dissolving the soluble support	48 hr (2880 min)
Preparing the surfaces	2 hr (120 min)
Total	**4 days 2 hr**

Note: The curing time for epoxy can be reduced from 24 hr to 4 hr by using an oven.

3.13 Injection Molding Setup

Since in this unique setup, the in-house developed injection machine [10] is directly mounted on the mold, the top mold box was designed in a way so that it could adapt the injection bushing in addition to the flange which holds the injection machine. Figure 3.26 shows the CAD design of the experimental setup.

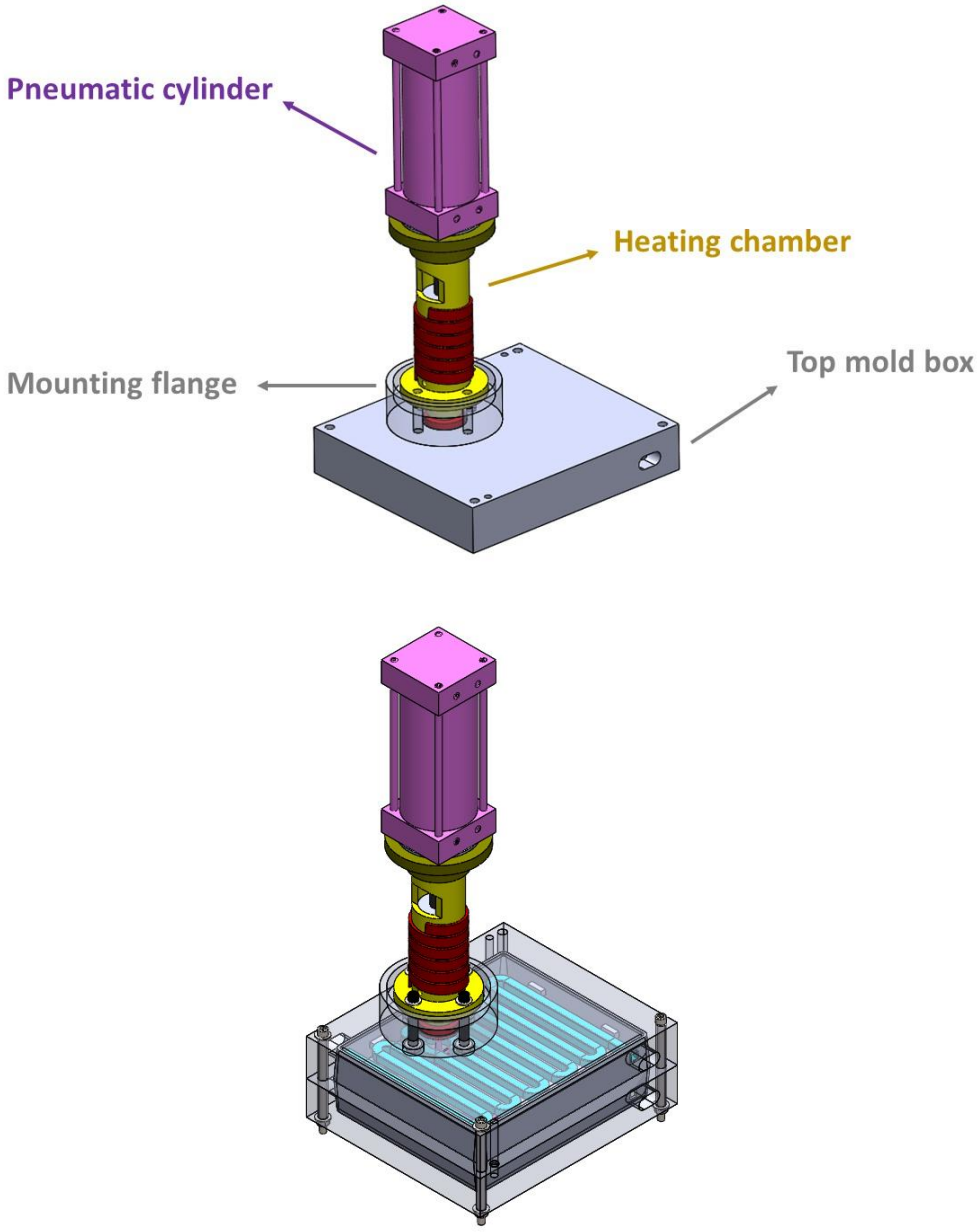

Figure 3.26 CAD design of the experimental setup

To complete the experimental setup, a centrifugal pump and a temperature control (developed in-house [10]) are required to complete the mold setup. Figure 3.27 shows the actual experimental set-up. The centrifugal pump was used to provide fluid flow inside the internal channels.

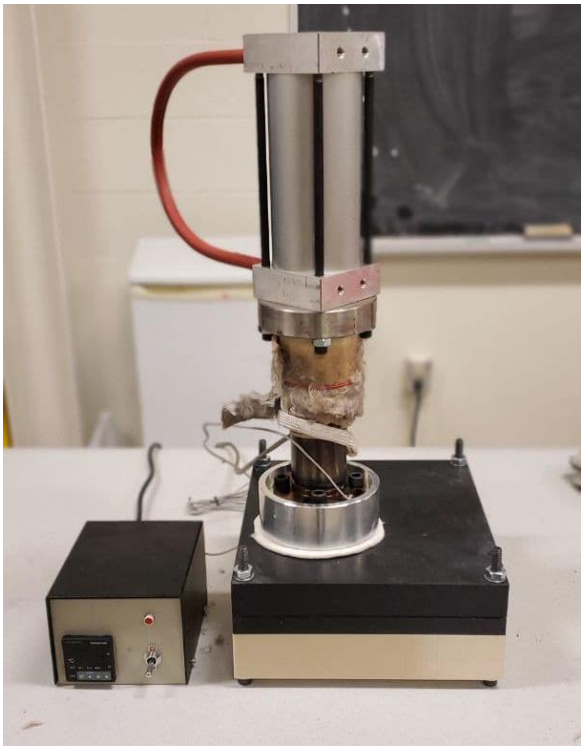

Figure 3.27 Experimental setup of the injection mold. The fluid inlets and outlets are not attached to the mold box here

To provide a flow of fluid inside the internal channels, a Mastercraft ¼ hp duel-function pump [29] was used. This pump can provide 101 lit/min in flow rate. The schematic of the fluid circuit has been provided in Figure 3.28.

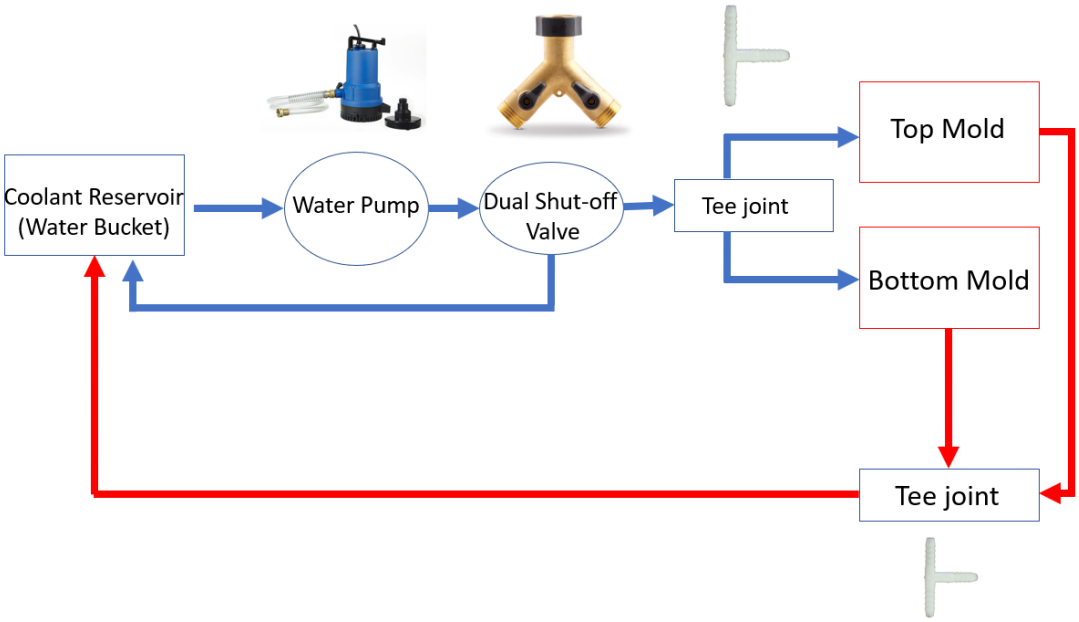

Figure 3.28 fluid circuit design for the developed injection setup

To inject the material, Technomelt-PA 7846 was used as the material of choice. The reasoning behind using Technomelt is that it is chemical resistant and does not absorb moisture and water. Additionally, Technomelt is a more resilient and stronger material than ABS and will not perform brittle behavior in case of any failure [25]. As a result, Technomelt would be a better candidate compared to ABS. ABS has a brittle behavior at room temperature and in case of any failure, it might cause some safety hazards to the end-user. Besides, ABS it is not resistant to the chemicals that might be used for cleaning the handles and it can also absorb moisture and water.

In the next section, the results are presented in detail.

CHAPTER 4

RESULTS AND DISCUSSION

4.1 Proof of Concept Results

As explained in section 3.3.2, two concept validation strategies were designed to evaluate the possibility of creating the developed tooling solution. In the first experiment, the possibility of building internal channels with complex geometries was studied. As demonstrated in Figure 4.1, the methodology developed in this research clearly shows that a complex internal cavity was created inside a curvilinear shape, and fluid was able to easily circulate inside the cast epoxy. As a result, any other internal geometry could be built with the same approach.

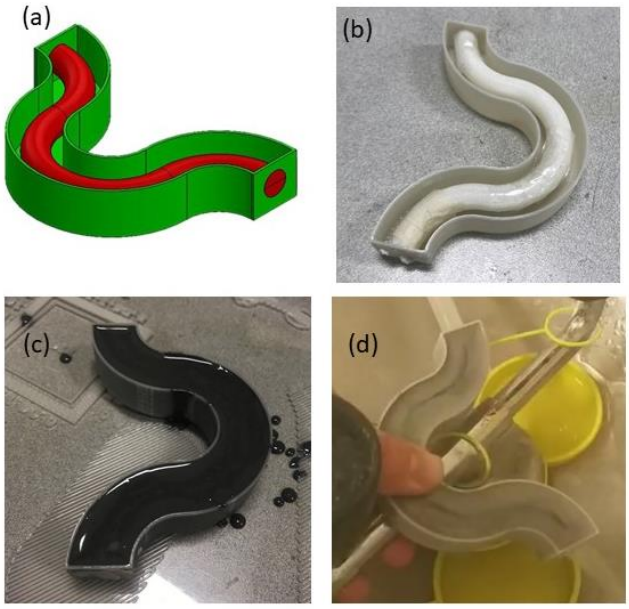

Figure 4.1 CAD design of the internal features experiment – the red section is made of soluble support material (a); Embedding the soluble support material(b); Pouring Epoxy Aremco 805 (c); After dissolving the support structure and testing the channel

In the second experiment, part ejection was studied. This test was conducted to evaluate the creation of cavities from soluble mold patterns, assess the effectiveness of the added draft angles, and test the mold release agent Demolub. Once the cavity was created, a layer of Demolub was sprayed on the cavity surface. The molten Technomelt was then poured

into the cavity and was solidified after several minutes. With the help of the added draft angles and also the application of Demolub, the test piece was effortlessly removed (see Figure 4.2). By successfully doing these two experiments, the main manufacturing concepts for the rapid tooling solution with special cooling channels were validated.

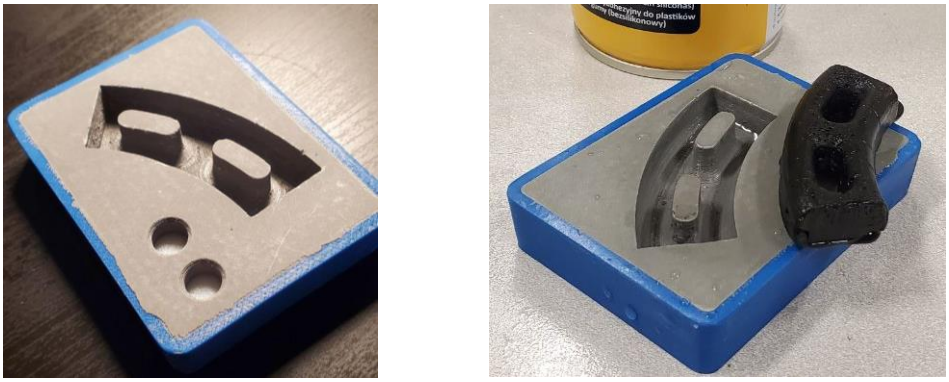

a) b)

Figure 4.2 Final release test mold (a); Test result of the release mold (b)

4.2 Limitations of Autodesk Moldflow

One of the limitations in Autodesk Moldflow was the restrictions in design for the cooling channels that had to be generated inside the software package. Since the geometry of cooling channels in Moldflow is only limited to circular and semi-circular cross-sections (see Figure 4.3), cooling channels with rectangular cross-sections could not be generated inside the software. Although the software allows the user to import external CAD designs for the cooling channels, it will not recognize rectangular components as a cooling feature, and they are defined as another cavity inside the simulation environment. Alternative simulation strategies / tools (such as COMSOL Multiphysics) and solution approaches need to be developed.

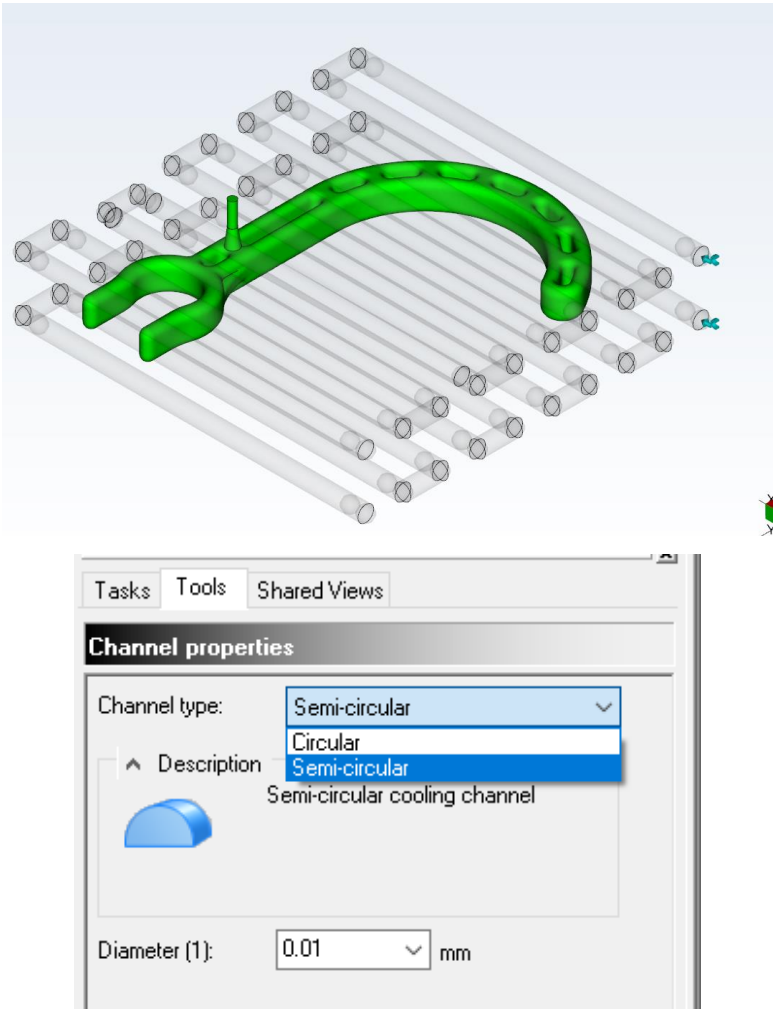

Figure 4.3 Cooling channel properties inside Autodesk Moldflow

4.3 Dissolving the Soluble Patterns.

After dissolving the sacrificial patterns made with SR-30, the surfaces of the cavities needed to be prepared. Sanding papers with high grit sizes (P800 and then P1200) were used to smooth out the surfaces of the cavities. The same operation was done to the molds to ensure that the top and bottom blocks will fit together perfectly. Figure 4.4 shows the cured, dissolved, and assembled versions of the cavity blocks.

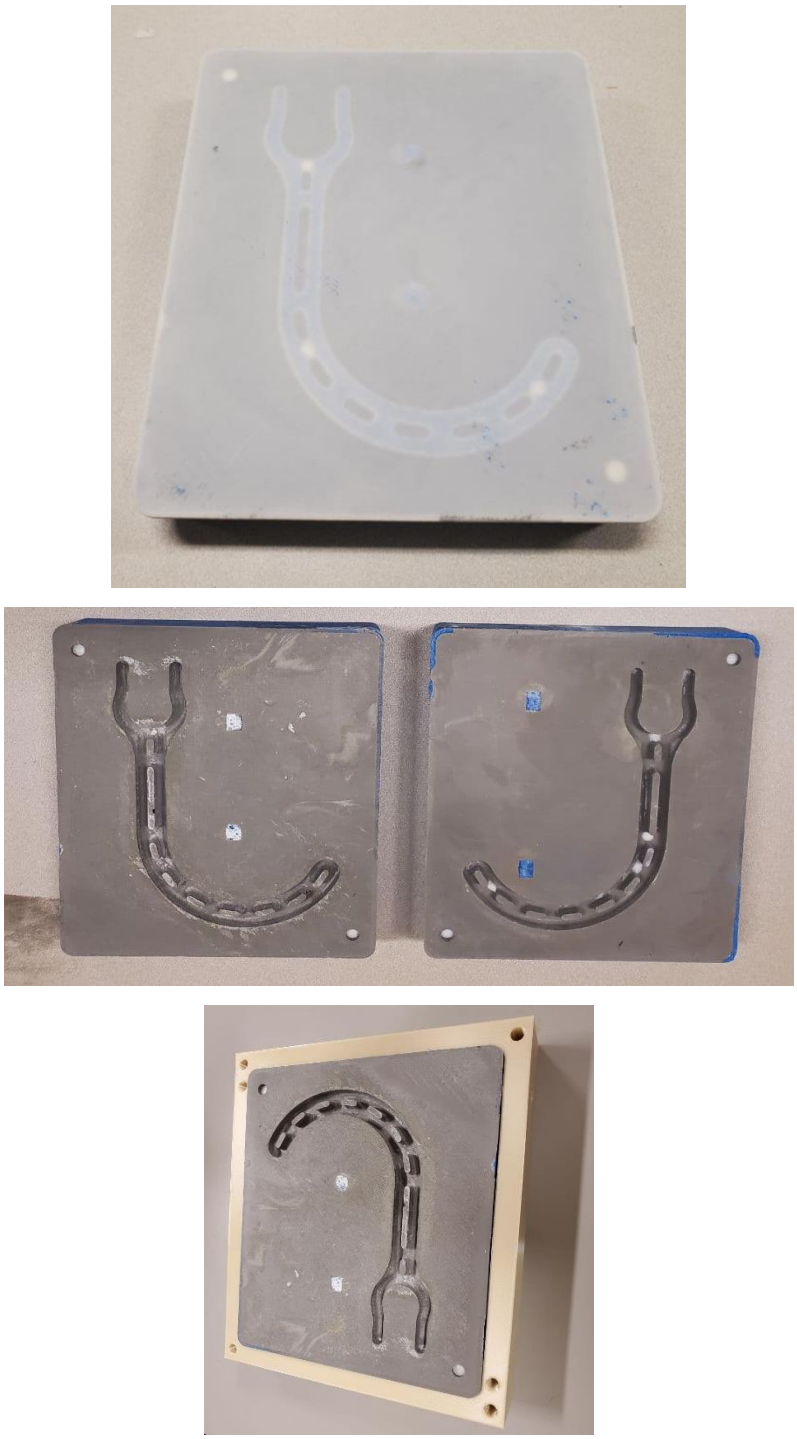

Figure 4.4 Cured epoxy (top); After dissolving the patterns (middle); And final assembled into mold box (bottom)

To connect the fluid circuit to the molds, additional ports were added on the side of the mold blocks. Special connectors were designed and built by FDM to connect the internal channels to the fluid circuit (see Figure 4.5). To test if the internal features were built without any internal issues, another fluid flow test was done and as shown in Figure 4.6, fluid was able to freely circulate inside the mold cavity. This test proved that the internal features were manufactured without any internal flaws or inconsistency.

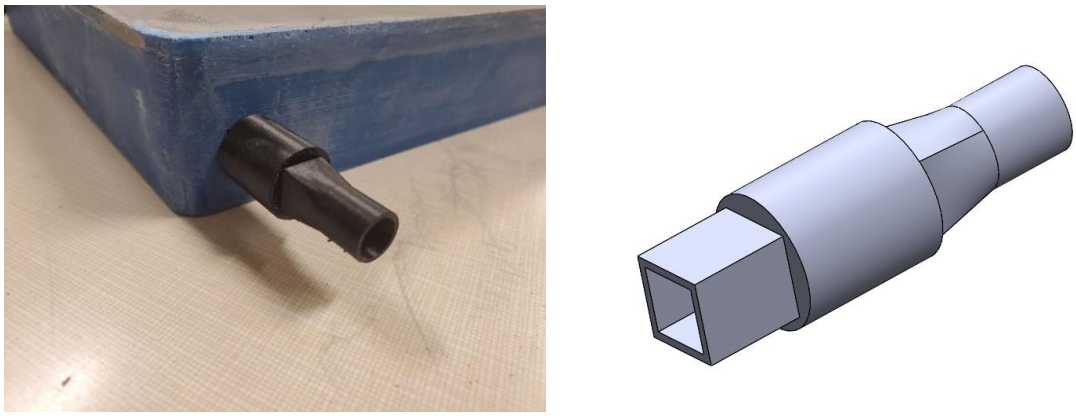

Figure 4.5 Connecting the fluid fittings to the internal features

Figure 4.6 Testing the fluid flow and connecting the mold to the fluid circuit

4.4 Injection Molding Results

Once all the components were ready, several layers of mold release agent were applied on the surface of the cavities and then the mold was assembled. By using four screws and two dowel pins, the mold boxes were aligned and fastened tightly. Next, pellets of Technomelt were poured into the heating chamber and the temperature of the machine was set to 200 ℃. Once the material reached the desired temperature, it was injected into the mold by the pneumatic cylinder. The part was cooled down for 1.5 minutes (according to the "time to eject" parameter in the simulations) while the fluid was circulating inside the internal channels. After 1.5 minutes the mold package was opened, and the component was easily removed from the cavities. Figure 4.7 shows the component inside the mold cavity. After the removal of the part, the excess material (flash) was removed, and the final product was successfully manufactured. (see Figure 4.8)

Figure 4.7 The injected J-hook right after opening the mold package (Red areas show the excess material "flash" that is inevitable an injection molding process)

Figure 4.8 Final J-hook after removal of the flash

4.4.1 Visual Assessment of the Injected J-hook

After removing the component from the mold, the injected J-hook was visually assessed and here are the key findings:

- Visually, it was clear that the cavity was completely filled and no underfilled area was observed. This validates the results of the injection simulation that stated the part was able to be filled completely and the component had a fill-confidence of 100%. (see Figure 4.9)

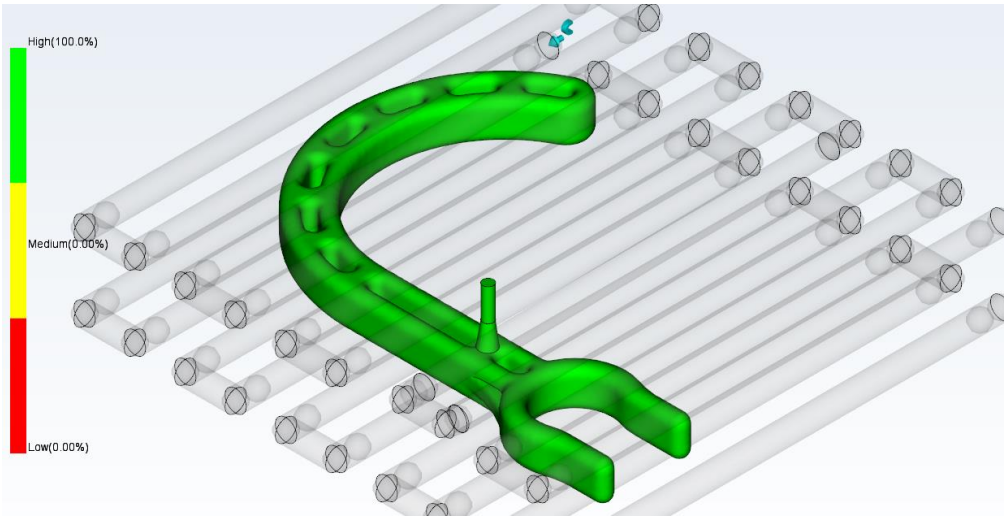

Figure 4.9 Confidence of fill from injection simulations in Autodesk Moldflow

- Due to the introduction of draft angles to the cavities (2 degrees) and the application of the silicone-free release agent Demolub, the part was effortlessly removed, and no scratch marks or surface defects were found on neither the J-hook nor the mold surfaces.
- After closely observing the surfaces of the J-hook under direct light, no sink mark was found on the surface of the product. This implies that the part was solidified uniformly. If any imbalance in filling and solidification happens within the injection process, it will result in sink marks and shrinkage. Inconsistent wall-thickness is another factor in forming sink marks on the surface of a component. Since one of the design decisions during the product design phase was to create gussets and islands in the middle of the J-hook, the lack of sink marks validates these design decisions.
- In addition to sink marks, weld-lines are another common defect in injection molded components that are easily visible by a standard visual test. The existence of weld-lines shows the area where molten material joined each other from different directions. Weld-lines and sink marks would suggest that there might be some design or process issues within the components. Once again, by not being able to observe any of these defects, design for manufacturing decisions for this component were further approved.
- Air bubbles are among the standard defects in an injection molding process. The existence of air bubbles, especially on the surfaces of a component would suggest that the air bubbles that might be formed during the melting stage of the pellets have not been able to escape the mold cavity. As shown in Figure 4.10, tiny air bubbles were formed on the upper end of the product surface. These air bubbles can be easily avoided by introducing air vents on the surface of the mold cavities. Adding air vents is a standard practice in injection molding and these air vents would enable the air bubbles to easily escape from the mold cavity. Figure 4.11 shows the suggested design of the air vents.

Figure 4.10 Formation of air bubbles at both ends of J-hook

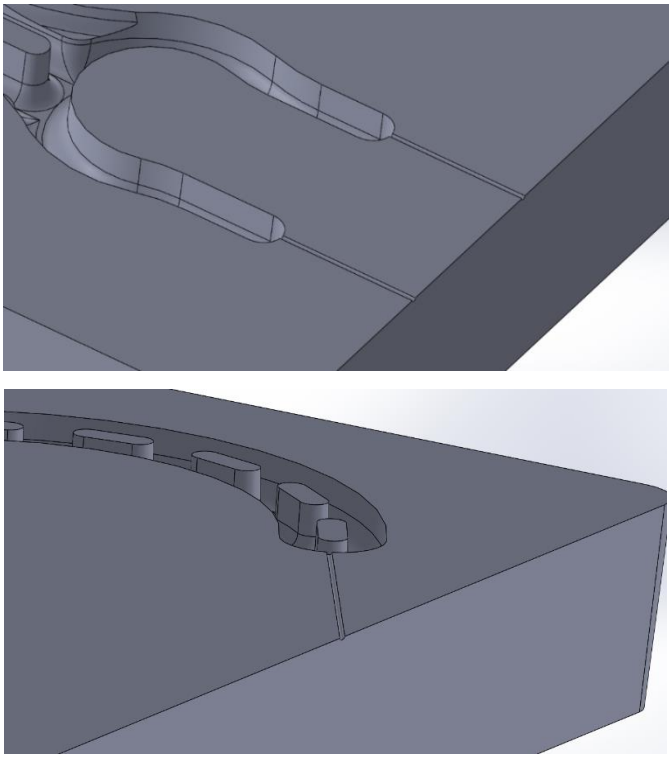

Figure 4.11 CAD design of the suggested air vents on cavity surface

4.4.2 Flatness Across the Length

To calculate the flatness and warpage of a component, a granite table and a dial indicator is a standard procedure. However, due to the limitation caused by the COVID-19

pandemic, access to such equipment was not available. As a result, the J-hook was placed on a relatively flat surface and light was reflected in the background. As shown in Figure 4.12, the light between the part and surface shows the warpage. A scale was placed next to the component to measure the warpage. The warpage was measured to be approximately around 1 mm across the length of the J-hook.

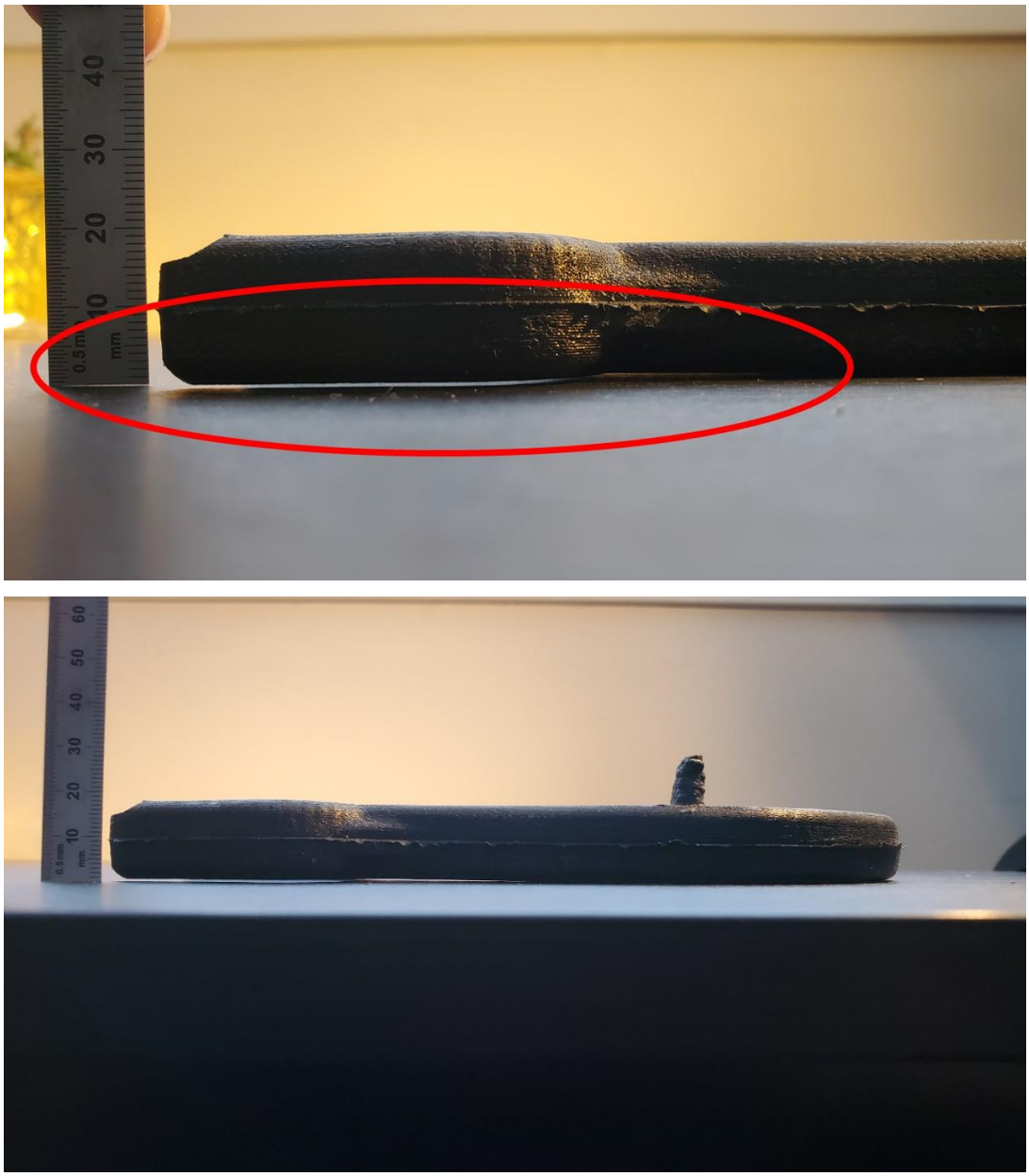

Figure 4.12 Measuring the flatness of the J-hook

4.4.3 Dimensional Error Along the J-hook

To evaluate the dimensional accuracy of the final product the width, height, and thickness of the injected J-hook were studied. In each orientation, three different areas were selected. Figure 4.13 shows these selected areas. From each section. three measurements were taken in a close proximity. Figure 4.14 shows how the width measurements were taken. Table 4.1 shows the measurements and calculations of the dimensional accuracy of width. The average dimension was calculated, and the results were compared to the original CAD file.

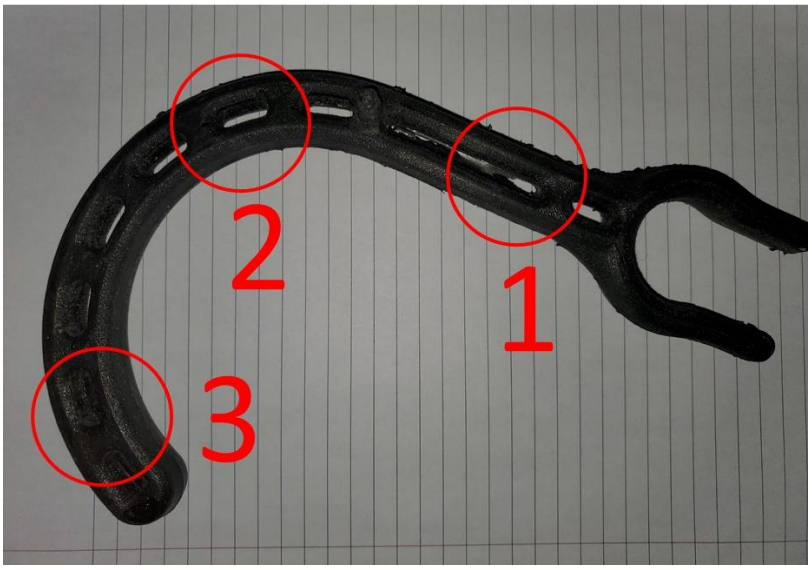

Figure 4.13 Selected areas for dimensional measurements

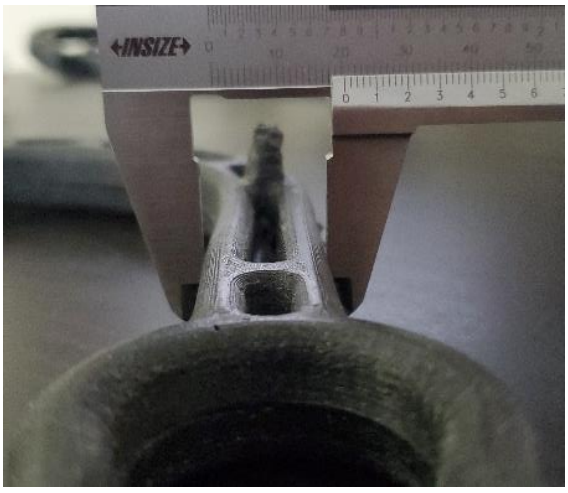

Figure 4.14 Measurement of part width via vernier caliper

Table 4.1 Width measurements and dimensional error calculations

Section	Measurement (mm)	Average (mm)	Original CAD (mm)	Error (±)
Area 1	20.60 20.65 20.45	20.56	20.87	1.48 %
Area 2	20.80 20.65 20.80	20.75	20.87	0.57 %
Area 3	20.45 20.45 20.80	20.57	20.87	1.43 %
			Average width error: 1.16 %	

The same measurements were taken from height of the part. Figure 4.15 shows how the height was measured. Table 4.2 shows the measurements and calculations.

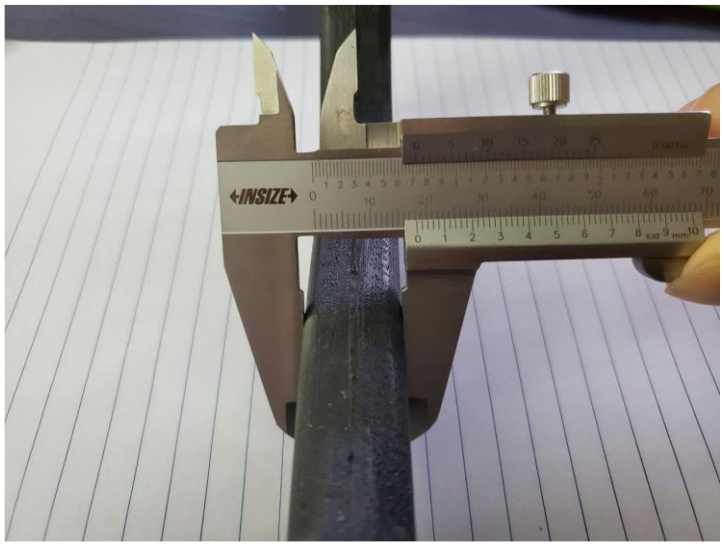

Figure 4.15 Measuring the height of the J-hook

Table 4.2 Height measurements and dimensional error calculations

Section	Measurement (mm)	Average (mm)	Original CAD (mm)	Error (±)
Area 1	18.20 18.20 18.20	18.2	18	1.11 %
Area 2	17.90 18.00 18.00	17.96	18	0.22 %
Area 3	17.85 18.00 17.90	17.91	18	0.5 %
			Average height error: 0.61 %	

To complete the measurements, the thickness of the mounting points, shown in Figure 4.16, were measured as well. Since there are two sides, three measurements were taken from each side of the mounting points. Table 4.3 shows the measurements and calculations of the mounting point thicknesses.

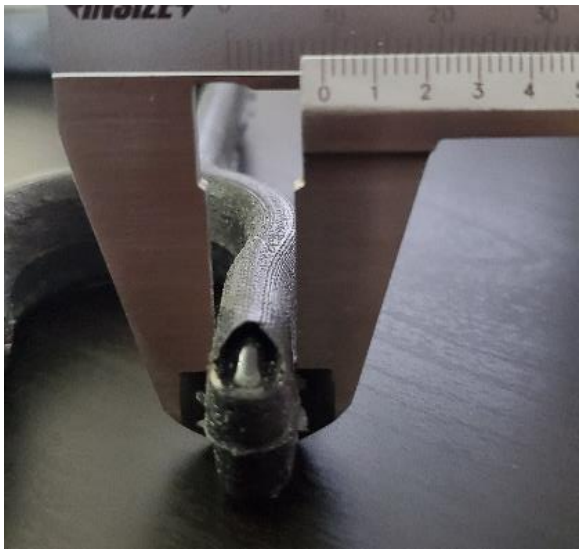

Figure 4.16 Measurements of the mounting point thicknesses

Table 4.3 Thickness measurements and dimensional error calculations of mounting points

Section	Measurement (mm)	Average (mm)	Original CAD (mm)	Error (±)
Left side	8.70 8.90 8.75	8.83	8.87	0.97%
Right side	8.90 9.05 9.00	8.98	8.87	1.24 %
			Average thickness error: 1.11 %	

As calculated in Tables 4.1, 4.2, and 4.3 the average error in different orientations of the component is around 1%. Considering the characteristics of the tooling (low-cost and low production time), the complex geometry of the final component , and the fact that normally the expected tolerances in injection molded components is between 0.05 – 0.1 mm [30], the dimensional accuracy of the process is acceptable.

To further validate the results, the arc of the J-hook was the next area of analysis. Figure 4.17 shows the area of interest. Since special measuring equipment was not available, image processing software, ImageJ was used to evaluate the dimensions of the inside and outside arc on the injected component. To begin the image processing, a high-quality image is required. In addition to a high-quality image, a measuring scale needs to be placed inside the image so that a precise scale can be defined inside the image processing software. As shown in Figure 4.18, a ruler was placed on top of the J-hook to set the scale. Once the scale was defined, several points were selected on the inside arc of the J-hook. Using the "fit circle" function in the software, a circle was fitted to the selected points. This process was repeated three times to make sure that the final measurement is more representative. Table 4.4 shows the measurements and calculations.

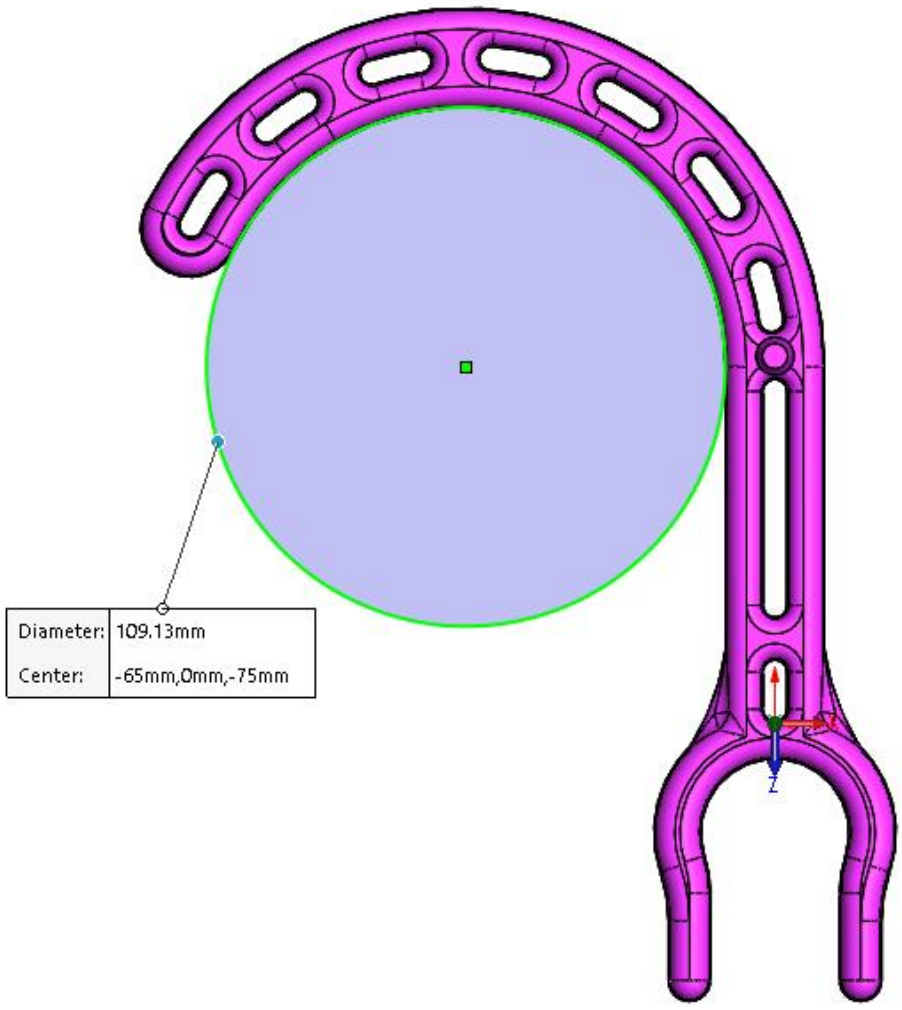

Figure 4.17 Inside arc of the J-hook in CAD software

Figure 4.18 The circle fitted to the inside arc by ImageJ software

Table 4.4 Calculating errors on the inside arc in ImageJ and CAD design

Measurements	**Dimensions (mm)**	**CAD Diameter (mm)**	**Error (±)**
First fit	Area: 9888.20 mm2 Dia.: 112.2 Perimeter: 352.50	Dia.: 109.13 Perimeter: 342.83	Dia.: 2.81 % Perimeter: 2.82%
Second fit	Area: 9849.00 mm2 Dia.: 111.98 Perimeter: 351.80	Dia.: 109.13 Perimeter: 342.83	Dia.: 2.61 % Perimeter: 2.61%
Third fit	Area: 9837.86 mm2 Dia.: 112.48 Perimeter: 353.38	Dia.: 109.13 Perimeter: 342.83	Dia.: 3.06 % Perimeter: 3.07%
		Ave. error in diameter: 2.82% **Ave. error in perimeter: 2.83 %**	

To further validate the arc dimensions, the same process was applied on the outer curve of the arc as well. Figure 4.19 shows the outer arc in Solidworks. Figure 4.20 shows a circle that was fitted to the points on the outside curve. Table 4.5 contains the measurements and calculations.

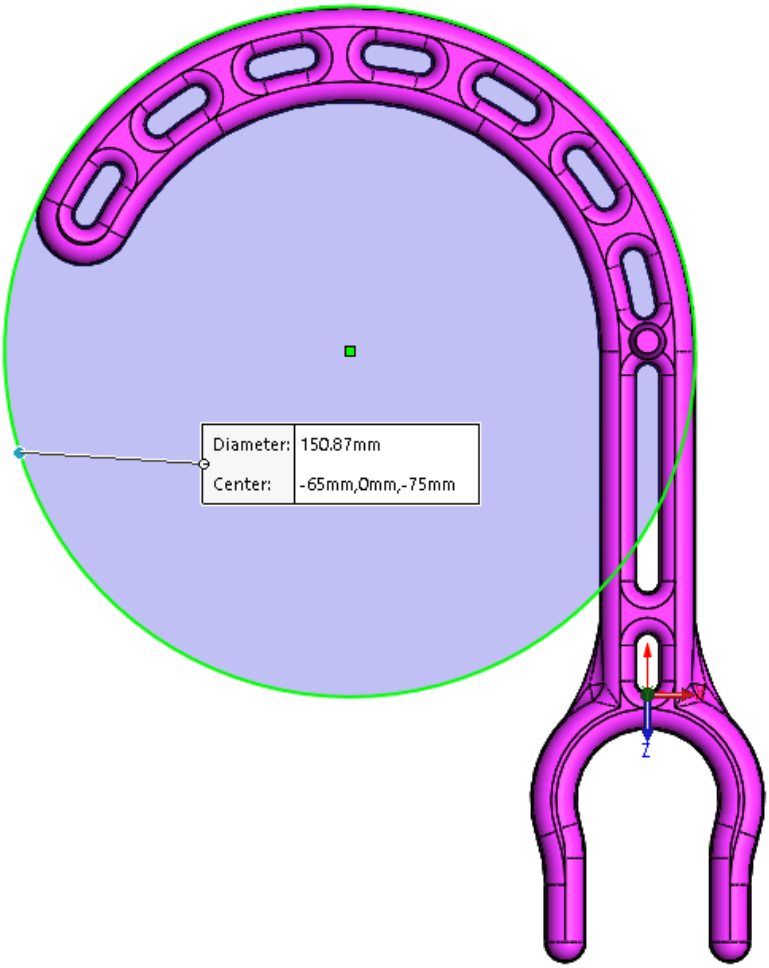

Figure 4.19 Outer diameter of the J-hook in Solidworks

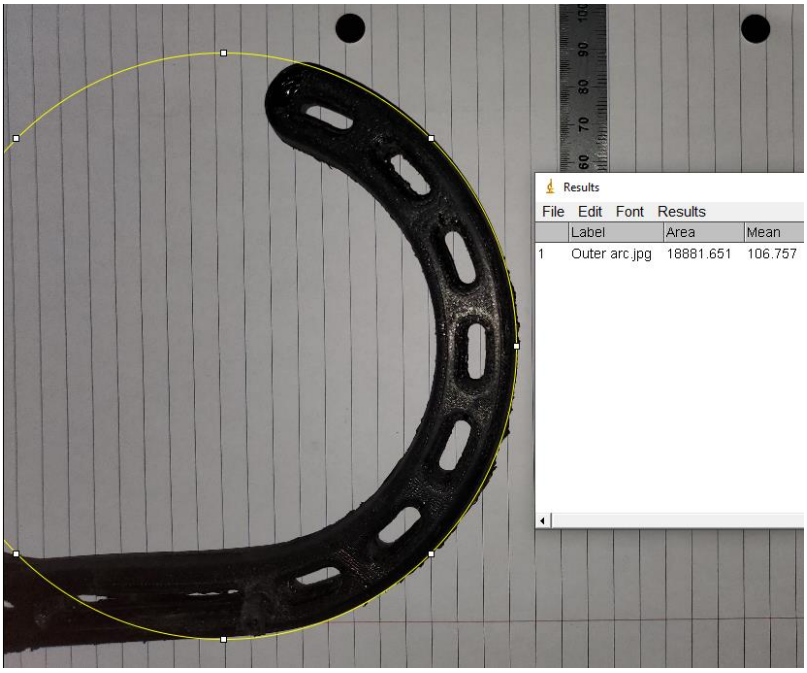

Figure 4.20 The circle fitted to the outer arc by ImageJ software

Table 4.5 Calculating errors on the outer arc in ImageJ and CAD design

Measurements	**Dimensions (mm)**	**CAD Diameter (mm)**	**Error (±)**
First fit	Area: 18860.21 mm2 Dia.: 154.96 Perimeter: 486.82	Dia.: 150.87 Perimeter: 473.99	Dia.: 2.71 % Perimeter: 2.70%
Second fit	Area: 18843.68 mm2 Dia.: 154.89 Perimeter: 486.61	Dia.: 150.87 Perimeter: 473.99	Dia.: 2.66 % Perimeter: 2.66%
Third fit	Area: 18881.65 mm2 Dia.: 155.05 Perimeter: 487.10	Dia.: 150.87 Perimeter: 473.99	Dia.: 2.77 % Perimeter: 2.77%
		Ave. error in diameter: 2.71% **Ave. error in perimeter: 2.71 %**	

By comparing the results, from the inner and outer calculations, the error in the arc section of the final product is almost 2.82 and 2.71%, respectively. Considering the dimensional accuracy across the different area of the part, the results of the injection molding is withing the desired tolerances. However, shape complexity and also the angles of the captured images might be contributing to the higher error percentage around the arcs.

4.3.4 Calculating the Flash.

To calculate the amount of material that was wasted in flash, the thickness of the excess material was measured via a Vernier caliper. Thickness of the flash was approximately 0.5 mm. Using image processing software, ImageJ, the surface area of the flash was calculated. To define a scale in the software, a known measurement was selected and that was used as a reference to calculate the area. (see Figure 4.21)

Figure 4.21 Setting a measurement scale for the flash calculation

This scale was selected due to its high contrast to the surrounding area. Based on the CAD design, this line was 17.5 mm. Figure 4.22 shows the measurements of flash in different

areas. The volume of flash in addition to the volume of material for the sprue, will show the amount of material that is wasted during each injection. By calculating the waste percentage, we are able to measure the efficiency of the solution.

Figure 4.22 Calculating the surface area of flash using ImageJ software

The total surface area for the flash was calculated to be around 3127.039 mm^2. By multiplying the area by the thickness of the flash, the volume of the flash was calculated at 1563.52 mm^3. In addition to the flash, the sprue needs to be counted as a waste material

as well, because it will be trimmed after the injection process. The total volume of the J-hook is 89535.66 mm^3.

As a result, the amount of material that is labeled as "waste' in each injection can be calculated. Table 4.6 shows the calculations. According to these numbers, in each injection approximately 2.4 % of material is wasted.

Table 4.6 Calculation of waste material volume fraction

J-hook material (product)	**Flash material (waste)**	**Sprue material (waste)**	**Total waste volume**
89,535.66 mm^3	1,563.52 mm^3	647.43 mm^3	**2,210.95** mm^3

4.5 Cost Analysis

Even though machining a metallic mold would have cost thousands of dollars with conventional methods - a similar mold for the glove remover was quoted for 60,000 CAD, the total cost of the developed tooling in this research was less than 500 CAD (summarized in Table 4.7). Since the durability and tool life of this developed tooling solution have not been established, more injections are required to evaluate tool life and calculate final piece price. Even if building additional rapid tools are needed to fulfill the production volume (low, low to medium, and medium production) the cost difference between machining a metallic mold and the low-cost solution developed tool in this research is still significant.

The developed tooling was built in less than 5 days whereas a machined mold would have taken several weeks to be completed. In addition, the internal channels would not have been able to be machined to the extent they were fabricated in this research. Building a J-hook with FDM technologies would have taken almost 3 hours to be fabricated. But by using this developed rapid tooling solution, the build time was reduced from 3 hours to less than 2 minutes per piece. Besides, the final material price was also reduced from 50 CAD for printing to less than 6 CAD for injection molding. By using the developed tooling solution, material price (Technomelt-PA) for other products developed during this research can be estimated. (refer to Table 4.8)

Table 4.7 Cost and time summary of the experiment set-up (for low to medium and medium production, extra epoxy molds might be needed to be built)

Component	Build time	Cost
Epoxy molds	~ 4 days & 8 hours	*330 CAD dollars
Ancillary hardware	-	Less than 50 CAD
Mold boxes	~18 hours	(Built from waste material)
Sacrificial patterns	~ 10 hours	Less than 100 CAD
		Total: 480 CAD

Table 4.8 Material cost comparison between FDM and IM for products using Technomelt-PA

Product	Cost for FDM (CAD $)	Cost for IM (CAD $)
Face shields	17.5	2.1
Door handle	50	6
Face mask	50.5	6.5
Glove remover	61.5	7.35

By optimizing the FDM process parameters, improving the CAD designs, and using an oven to cure the epoxy, the production time of the components can be reduced by 24 hours. Table 4.9 demonstrates the new and optimized fabrication time for the same experimental setup. Additionally, if a set of permanent mold boxes are machined from a metallic material, e.g. Aluminum, the build time of the mold boxes is eliminated from future experiments. Since the inserts can be swapped with other product inserts, this adds another level of versatility to this low-cost solution. The application of topology optimization strategies can remove the unnecessary material from the inserts, reduce the amount of epoxy that is needed, and Consequently, the cost of epoxy for the inserts can be further reduced for future experiments.

The result summary, conclusions and future studies are further discussed in chapter 5.

Table 4.9 Build time information of the optimized fabrication for the low-cost tooling setup

Process	**Time**
Printing the soluble top Pattern (SR-30)	2 hr 33 min (153 min)
Printing the soluble bottom pattern (SR-30)	2 hr 53 min (173 min)
Printing two surrounding enclosures (ABS)	7 hr 20 min (440 min)
Printing two internal soluble patterns (SR-30)	3 hr 28 min (208 min)
Epoxy casting and cure time (both made at the same time) – using an oven	8 hr (480 min)
Dissolving the soluble support	48 hr (2880 min)
Preparing the surfaces	2 hr (120 min)
Total	**3 days 2 hr**

CHAPTER 5
CONCLUSION AND FUTURE WORKS

5.1 Conclusion

In this research, a low-cost rapid tooling solution was developed and tested. In this tooling solution, internal features were manufactured by using soluble materials. These internal features were built without any additional support structures. Building internal features inside a tool is restricted by the linear nature of conventional machining process, and advanced manufacturing solutions such as metal additive manufacturing are very expensive and require additional support structures for internal channels. A low cost solution that is able to build complex internal features, can open up new opportunities for researchers to conduct heat modelling and design an efficient cooling design.

Since a complex 2D channel design was able to be manufactured by this low-cost solution, any similar 2D pattern could be easily built following the developed methodology in this research.

The objective of this study, that is the development of a rapid low-cost solution was met, and the cost of the material and manufacturing time was reduced significantly. In this research, the build time for the J-hook was significantly reduced from 3 hours (FDM) to less than 2 minutes (IM). From the cost analysis conducted, less than 500 CAD was used to build this tooling setup and the material cost of the J-hook was reduced from 50 CAD to less than 6 CAD. To calculate the final cost of the product, more injections need to be done to test the durability of this developed tooling, then a final cost per piece can be estimated. Additionally, by using IM process instead of AM, more injection material is available to fabricate the product.

Building complex cooling channels with metal additive manufacturing technologies not only is costly but also has geometry limitations. For example, building internal channels with rectangular cross-sections would require internal support structures and having a support structure would disrupt the coolant flow inside the channels. By following the design for manufacturing approaches (split design) developed in this research, highly

complex cooling channels with different cross-sections can be built and incorporated inside a tool in a timely and cost-effective manner.

All of the results show that the objectives of this research were met and a low-cost rapid solution with internal channels was developed and the end result was a successfully manufactured component with complex geometry and dimensional error of approximately 1% to 3%.

Finally, one of the obstacles that was encountered during this research, was software limitations of Autodesk Moldflow. This limitation would not allow the user to generate rectangular cooling channels. To leverage alternative designs developed in this study, the tools available to manufacturers need to be upgraded.

5.2 Future Work

- Since a very complex 2D planar internal feature was manufactured by using the proposed solution, next steps include building more complex internal channels with:
    - variable cross section geometries and
    - complex 3D (non-planar) features

To evaluate the flexibility and also extendibility of this developed solution, two proof of concept tests have been designed. Two channel designs with a variable cross-section (Figure 5.1) and non-planar geometry (Figure 5.2) have been designed and tested. By successfully designing and building these proof-of-concept experiments, it has been demonstrated that the developed methodology in this research is highly extendable and any complex channel design can be fabricated and incorporated into a mold without any significant design limitation and support structure.

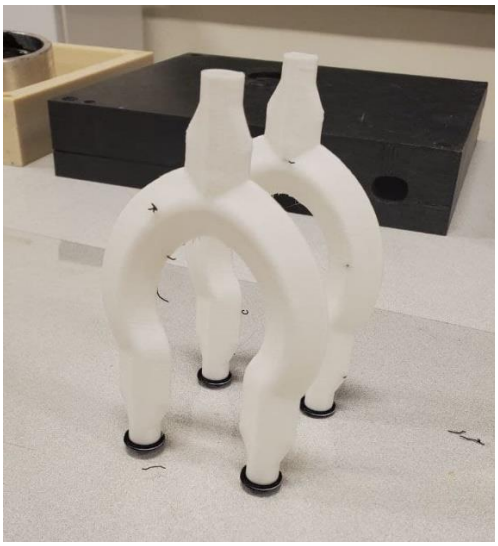

a)

b)

c)

d)

Figure 5.1 Soluble channel with variable cross section without any support material (a); Assembling the test piece (b); Casting Aremco 805 (c); Successfully testing fluid flow (d)

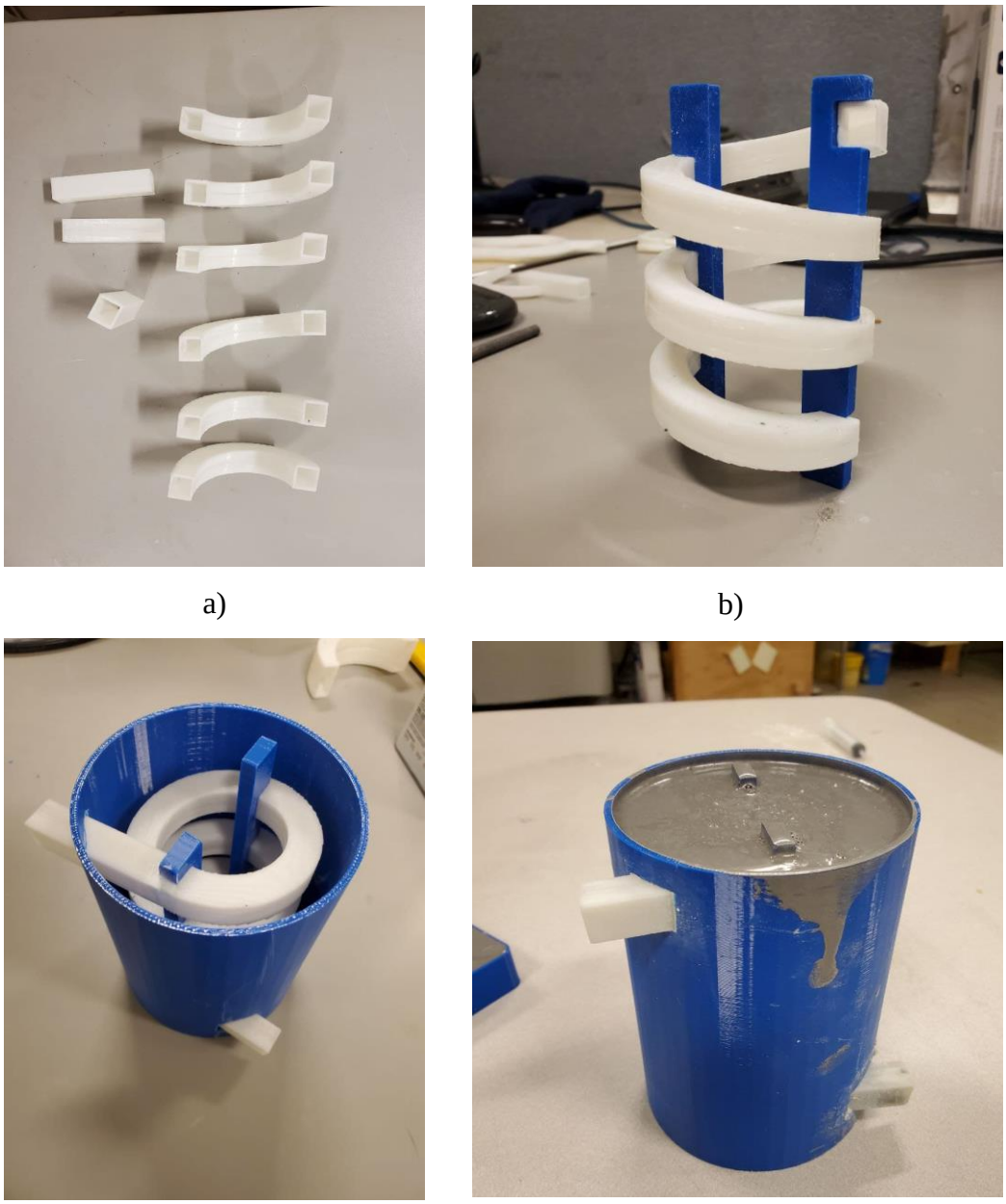

a) b)

c) d)

Figure 5.2 Non-planar cooling channel design with modular design (a): Assembling the modules and creating a spiral channel (b); Assembling the test components (c); Casting Aremco 805 (d)

- Using the methodology and design approaches developed in this work provide a good opportunity to develop a heat model to conduct virtual heat analysis and fluid modeling. These optimizations can help maximize the cooling capacity, efficiency, and design of

these internal channels to build working and effective cooling channels. Based on the results of this research, fabricating experimental test setups can be significantly reduced. As reported by the reviewed literature for this work, the high cost of metal additive manufacturing was a limiting factor in conduction experimental heat and fluid flow studies. In future research, heat transfer analysis will be conducted to improve the designs of internal features. Additionally, different epoxies and other production ideas such as using metallic chills or sensors that are embedded inside the tools, can be easily incorporated in this tooling solution. This will help derive great experimental data sets that can help optimize alternative cooling designs.

- Since building complex geometries by metal additive manufacturing requires support material, it will introduce interference issues inside the channels. A new and unique internal feature has been developed to be manufactured by hybrid additive manufacturing technologies. This part has been designed to be manufacturable via 3-axis metal deposition machine. This metallic tooling is currently under development and will be built in near future. (Figure 5.3)

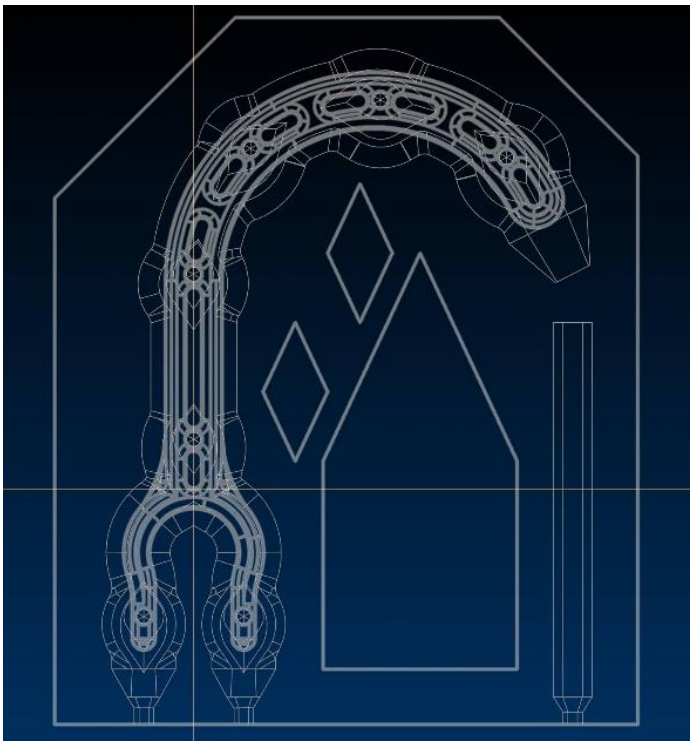

Figure 5.3 The developed internal design for 3-axis metal additive manufacturing

REFERENCES/BIBLIOGRAPHY

[1] "BC Center for Disease Control - About Covid-19," 2019. [Online]. Available: http://www.bccdc.ca/health-info/diseases-conditions/covid-19/about-covid-19. [Accessed 10 October 2020].

[2] W. H. Organization, "Coronavirus disease 2019 (COVID-19)Situation Report – 73," 2 April 2020. [Online]. Available: https://www.who.int/docs/default-source/coronaviruse/situation-reports/20200402-sitrep-73-covid-19.pdf?sfvrsn=5ae25bc7_6. [Accessed 10 October 2020].

[3] Centers for Disease Control and Prevention, "How COVID-19 Spreads," 28 October 2020. [Online]. Available: https://www.cdc.gov/coronavirus/2019-ncov/prevent-getting-sick/how-covid-spreads.html. [Accessed 5 February 2021].

[4] Turng, L., Chen, S., Advanced Injection Molding Technologies, Munich; Cincinnati: Hanser, 2019.

[5] Dimla, D. E., Camilotto, M., Miani, F. , "Design and optimisation of conformal cooling channels in injection moulding tools," *Journal of Materials Processing Technology,* vol. 164, no. 165, pp. 1294-1300, 2005.

[6] Kazmer, D., Injection mold design engineering, Munich, Germany ; Cincinnati, Ohio : Hanser Publications, 2016.

[7] "Sink marks and voids," [Online]. Available: https://www.dc.engr.scu.edu/cmdoc/dg_doc/develop/trouble/sinkmark/f5000001.htm. [Accessed 4 February 2021].

[8] ISO/ASTM 52900, "ISO/ASTM 52900, Additive manufacturing - General principles - terminology," ISO, 2015. [Online]. Available:

https://www.iso.org/obp/ui/#iso:std:iso-astm:52900:dis:ed-2:v1:en. [Accessed 21 1 2021].

[9] Urbanic, R. J., Hedrick, R., "Fused deposition modeling design rules for building large, complex components," *Caomputer-aided design & applications,* vol. 13, no. 3, pp. 348-368, 2016.

[10] Kalami, H., Urbanic, R. J., "Design and Fabrication of a Low Volume, High Temperature Injection Mould Leveraging a Rapid Tooling Approach," *Int. Journal of Advanced Manufacturing Technology, Special Issue - Digital Manufacturing & Assembly Systems*, 2019. https://doi.org/10.1007/s00170-019-03799-8.

[11] Tan, C., Wang, D., Ma, W., Chen, Y., Chen, S., Yang, Y., Zhou, K., "Design and additive manufacturing of novel conformal cooling molds," *Materials & Design,* vol. 196, 2020.

[12] C. K. Chua, K. F. Leong, C. S. Lim, "FDM 3D printing technology in manufacturing composite elements," *Archives of Metallurgy and Materials,* vol. 58, no. 4, pp. 1415-1418, 2013.

[13] Stratasys, "FDM Materials," [Online]. Available: https://www.stratasys.com/materials/search?technologies=ff37d7b8297c4e43977c155d765f3305&sortIndex=0. [Accessed 29 12 2020].

[14] Stratasys, " FDM Support Materials," Stratasys, [Online]. Available: https://support.stratasys.com/en/materials/fdm/fdm-support-materials. [Accessed 8 1 2021].

[15] Levy, G. N., Schnidel, R., Kruth, J. P., "RAPID MANUFACTURING AND RAPID TOOLING WITH LAYER MANUFACTURING (LM) TECHNOLOGIES, STATE OF THE ART AND FUTURE PERSPECTIVES," *CIRP Annals,* vol. 52, no. 2, pp. 589-609, 2003.

[16] Karapatis, N. P., van Griethuysen, J. P. S., Glardon, R., "Direct rapid tooling: a review of current research," *Rapid prototyping Journal,* vol. 4, no. 2, pp. 77-89, 1998.

[17] Akula, S., Karunakaran, K. P.,, "Hybrid adaptive layer manufacturing: An Intelligent art of direct metal rapid tooling process," *Robotics and Computer-Integrated Manufacturing,* vol. 22, no. 2, pp. 113-123, 2006.

[18] Sachs, E., Wylonis, E., Allen, S., Cima, M., Guo, H., "Production of injection molding tooling with conformal cooling channels using the three dimensional printing process.," *Polymer Engineering & Science,* vol. 40, pp. 1232-1247, 2000.

[19] Wu, T., jahan, S. A., Kumaar, P., Tovar, A., El-Mounayri, H., Zhang, y., Zhang, J., Acheson, D., Brand, K., Nalim, R., ", A Framework for optimizing the design of injection molds with conformal cooling for additive manufacturing," *Procedia Manufacturing,* vol. 1, pp. 404-415, 2015.

[20] Shinde, M. S., & Ashtankar, K. M. , "Additive manufacturing–assisted conformal cooling channels in mold manufacturing processes," *Advances in Mechanical Engineering,* 2017.

[21] Jahan, S. A., El-Mounayri, H., "Optimal Conformal Cooling Channels in 3D Printed Dies for Plastic Injection Molding," *Procedia Manufacturing,* vol. 5, pp. 888-900, 2016.

[22] Mazur, M., Leary, M., McMillan, M., Elambasseril, J. and Brandt, M., "SLM additive manufacture of H13 tool steel with conformal cooling and structural lattices," *Rapid Prototyping Journal,* vol. 22, no. 3, pp. 504-5018, 2016.

[23] B. Mohajernia, Investigation of methods and validation techniques for plastic injection mold weight reduction, Windsor: University of Windsor, 2015.

[24] Jeff Gardiner, "Finite Element Analysis Convergence and Mesh Independence," 27 March 2017. [Online]. Available: https://www.xceed-eng.com/finite-element-analysis-convergence-and-mesh-independence/. [Accessed 18 March 2021].

[25] Ellsworth Adhesives, "Technomelt," [Online]. Available: https://www.ellsworth.com/globalassets/literature-library/manufacturer/henkel-loctite/henkel-loctite-brochure-technomelt-one-step-molding-products.pdf. [Accessed 18 Mar 2021].

[26] Aremco Products, Inc. , "Aremco-Bond™ 805 Epoxy for Bonding and Molding Applications," [Online]. Available: http://www.graphitestore.com/core/media/media.nl?id=9825&c=4343521&h=5a89fef6d5dbea0a86d4. [Accessed 17 09 2020].

[27] Silicone-free mould release agent, "Silicone-free mould release agent," Molydal, [Online]. Available: https://www.molydal.com/en/products/lubricants/plastic-injection/mould-release-agents/silicone-free-mould-release-agent/demolub.html. [Accessed 7 1 2021].

[28] DAP, "'33'® Window Glazing," [Online]. Available: https://www.dap.com/products-projects/product-categories/patch-repair/glazing/33-glazing/. [Accessed 15 March 2021].

[29] Canadia Tire, "Mastercraft 1/4-HP Duel Function Pump," [Online]. Available: https://www.canadiantire.ca/en/pdp/mastercraft-1-4-hp-duel-function-pump-0623408p.html. [Accessed 15 March 2021].

[30] Dong Guan Sincere Tech, "Precision Plastic Injection Molding," 1 january 2020. [Online]. Available: https://www.plasticmold.net/precision-plastic-injection-molding/. [Accessed 2021 April 10].

APPENDICES

Appendix A: Door handle designs

Different door handle solutions were designed during this research and the designs are shown in the following figures.

Figure A.1 First extended version of J-hook door handle

a)

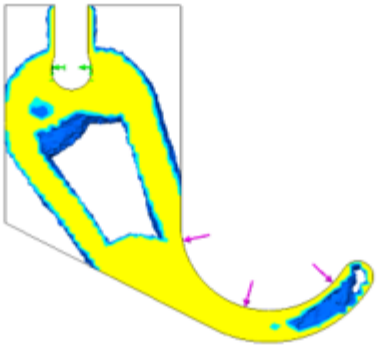

b)

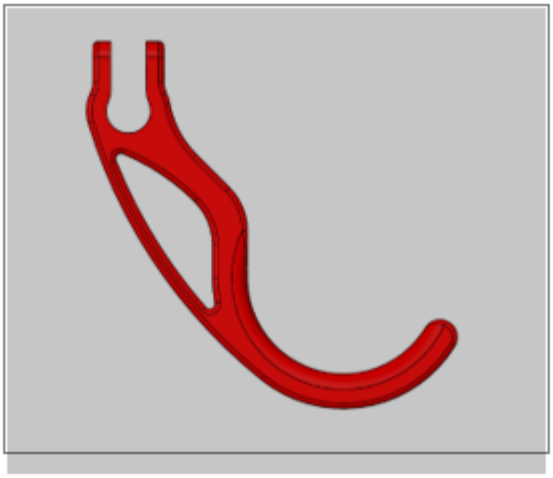

c)

Figure A.2 new design after applying topology optimization

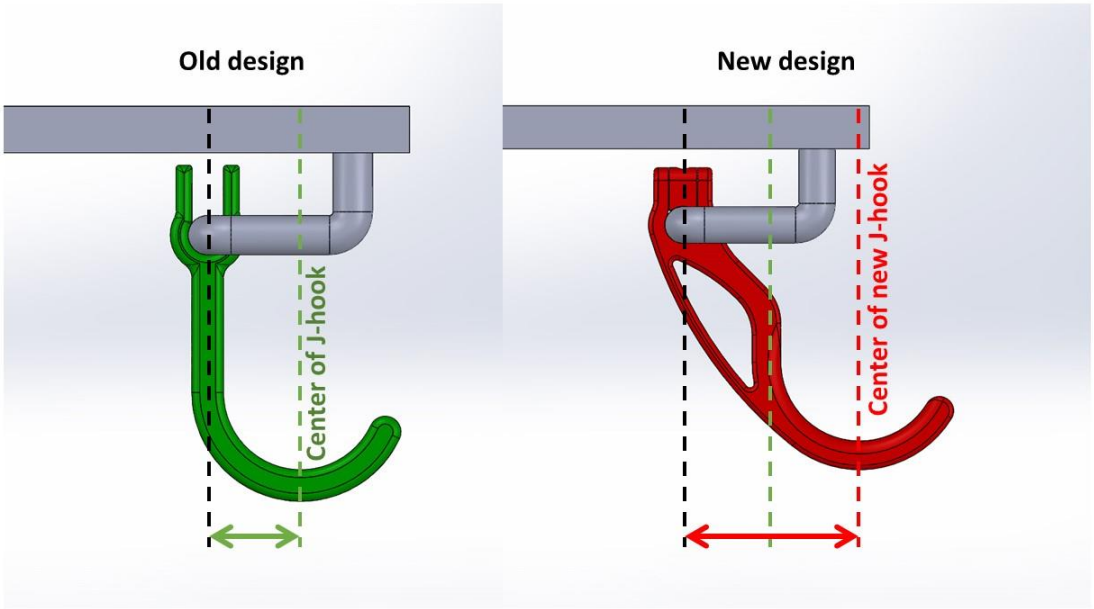

Figure A.3 First version and final version of extended J-hook

Figure A.4 Version 1 of type II door handle

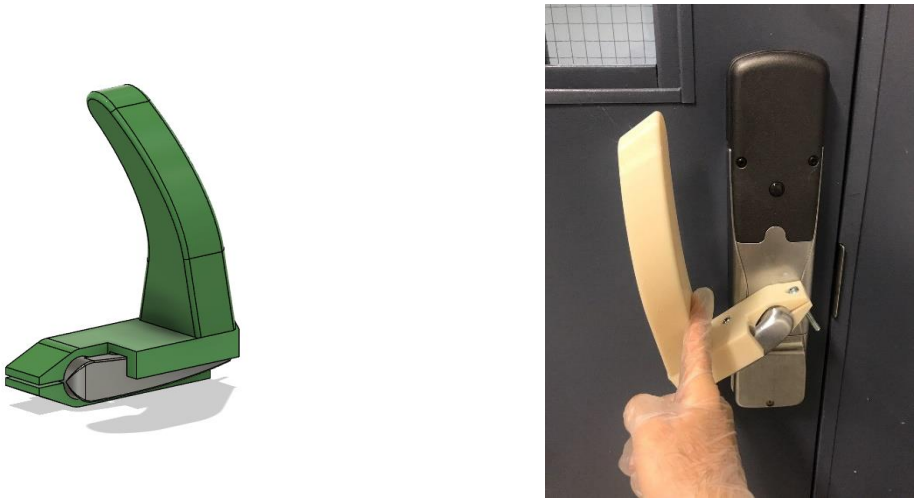

Figure A.5 Version 2 of type II door handles

Figure A.6 Version 3 of type II door handle design

Figure A.7 Two of the most common type III doorknobs.

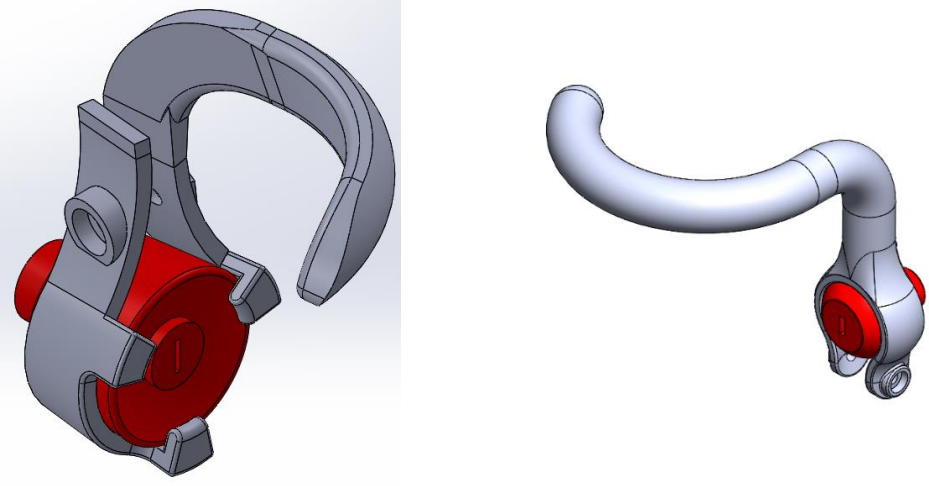

Figure A.8 CAD designs of type III door handle

Appendix B: Face shield design

Design features of the adaptive face shield have been demonstrated here. It has a fixed top which holds the shield and has an adaptive base which is designed to adapt different forehead shapes and sizes. This product was designed by Hamed Kalami.

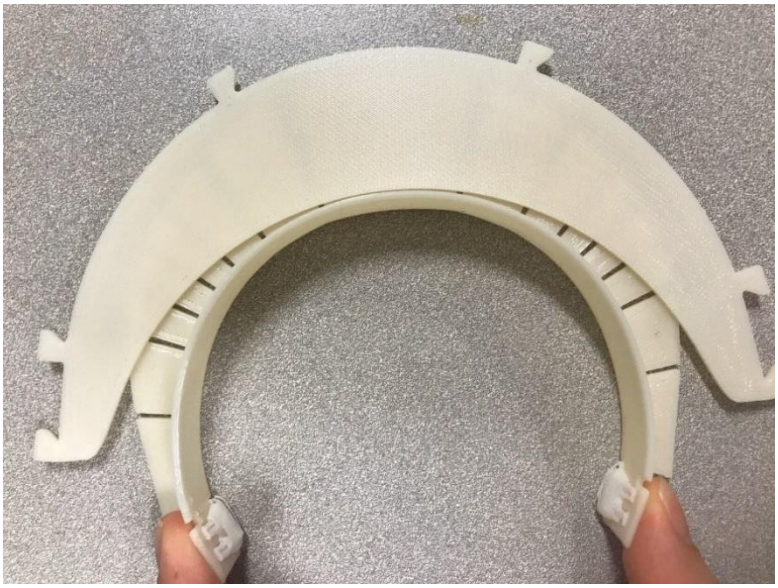

Figure B.1 Adaptability of the face shield top

Figure B.2 Full version of the face shield

Appendix C: Adaptive face mask

Design features of Face mask have been demonstrated here. This design was created in close cooperation with Hamoon Ramezani. In this design an easy release filter casing was designed into the product. A special silicone gasket was designed in order to create a better sealing around user's face. Having this gasket can also reduce the pressure on user's face and reduce fatigue after hours of usage.

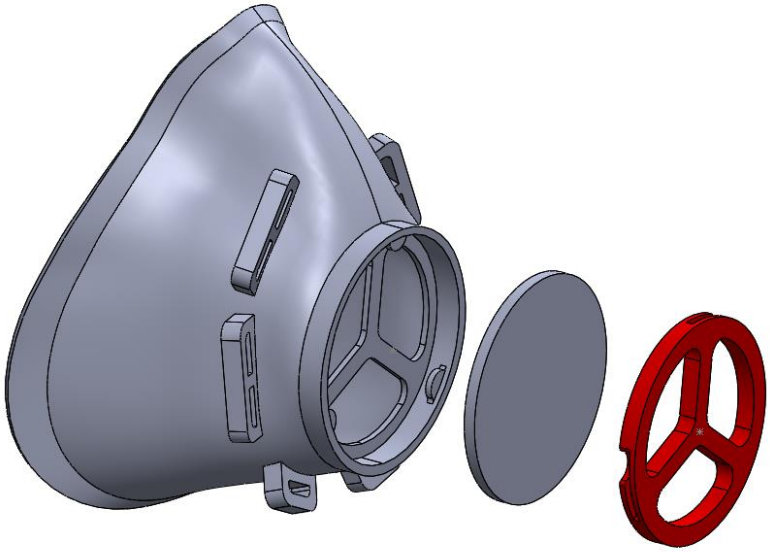

Figure C.1 CAD design of the face mask with filter and easy release cap

Figure C.2 Final design of the face mask.

Appendix D: Hands free glove remover

This product is designed to help users remove their infected gloves without using their fingers. This product can help reduce contamination on hands. This design was designed by Mohamad Najimi however topology optimization and manufacturing steps were taken as a part of this thesis.

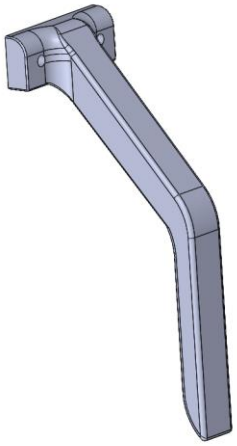

Figure D.1 First version of hands-free glove remover

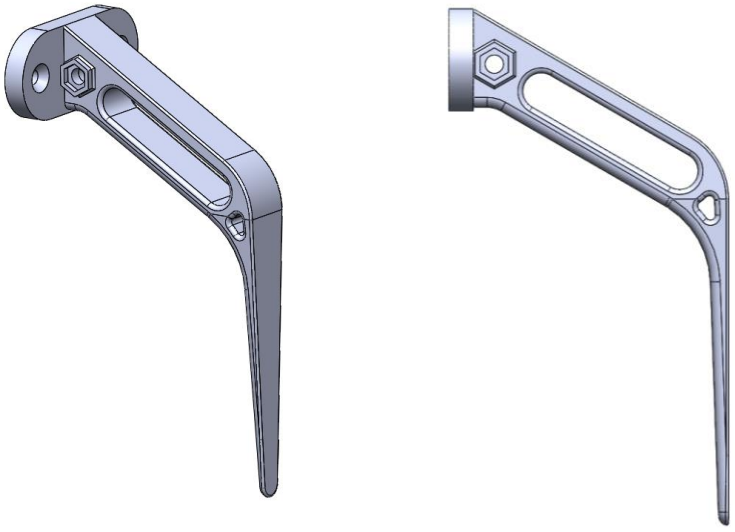

Figure D.2 Topology optimized and final version of hands-free glove remover

VITA AUCTORIS

NAME:	Alireza Davoud Pasha
PLACE OF BIRTH:	Ahvaz, Iran
YEAR OF BIRTH:	1995
EDUCATION:	Sharif High School, Karaj, Iran, 2013
	Azad University of Karaj, B.Sc., Iran, 2017
	University of Windsor, M.Sc., Windsor, ON, 2021